PHYSICAL REVIEW D **78,** 104028 (2008)

Perturbation method for classical spinning particle motion. I. Kerr space-time

Dinesh Singh*

Department of Physics, University of Regina, Regina, Saskatchewan, S4S 0A2, Canada

(Received 22 August 2008; published 25 November 2008)

This paper presents an analytic perturbation approach to the dynamics of a classical spinning particle, according to the Mathisson-Papapetrou-Dixon (MPD) equations of motion, with a direct application to circular motion around a Kerr black hole. The formalism is established in terms of a power series expansion with respect to the particle's spin magnitude, where the particle's kinematic and dynamical degrees are expressed in a completely general form that can be constructed to infinite order in the expansion parameter. It is further shown that the particle's squared mass and spin magnitude can shift due to a classical analogue of radiative corrections that arise from spin-curvature coupling. Explicit expressions are determined for the case of circular motion near the event horizon a Kerr black hole, where the mass and spin shift contributions are dependent on the initial conditions of the particle's spin orientation. A preliminary analysis of the stability properties of the orbital motion in the Kerr background due to spin-curvature interactions is explored and briefly discussed.

DOI: 10.1103/PhysRevD.78.104028 PACS numbers: 04.20.Cv, 04.25.−g, 04.70.Bw

I. INTRODUCTION

One of the earliest and ongoing research interests in general relativity concerns the dynamics of extended bodies in the presence of strong gravitational backgrounds. Considering that virtually all astrophysical objects in the Universe, such as black holes, neutron stars, and other isolated massive bodies, have at least some spin angular momentum in their formation, it is not difficult to surmise that an in-depth study of moving relativistic systems with spin is a useful endeavour. A relevant example concerns the motion of rapidly rotating neutron stars in circular orbit around supermassive black holes like ones believed to exist in the center of galaxies, which serve as candidate sources for emitting low-frequency gravitational wave radiation that may be detected by the space-based LISA gravitational wave observatory [1].

A first attempt to understand the dynamics of extended bodies in curved space-time was put forward by Mathisson [2], who showed the existence of an interaction term involving the direct coupling of particle spin to the Riemann curvature tensor generated by a background source. Steady progress was made since this first attempt, with a notable contribution made several years afterwards by Papapetrou [3], who proposed that the spinning particle exists within a space-time world tube containing its center-of-mass worldline, where its associated matter field has compact support. In addition, multipole moment contributions, i.e. beyond the mass monopole and spin dipole, to the extended objects full equations of motion were considered by Tulczyjew [4] and others, ultimately leading to the expressions obtained by Dixon [5,6], with a self-consistent description for all multipole moment contributions to infinite order. While the various theories of extended body motion in curved space-time differ with respect to the higher-order multipole moments, all of them recover the ''pole-dipole approximation'' identified initially by Mathisson and Papapetrou, which are satisfactory for most practical calculations, so long as the dimensions of the spinning body are small when compared to the background space-time's local radius of curvature. These truncated expressions of the full equations of motion are commonly known as the Mathisson-Papapetrou-Dixon (MPD) equations.

There has been widespread interest in applying the MPD equations to the dynamics of classical spinning particles in orbit around rotating black holes, as described by the Kerr metric [7–11]. In many ways, the Kerr background is an ideal testing ground for the MPD equations, since both mass sources are spinning, which introduce interesting spin-curvature effects that impact upon the orbiting particle's overall evolution. Furthermore, it lends itself well to numerical simulations of deterministic chaos under extreme conditions [11–14], as well as studies of gravitational wave generation [15,16] arising from spin-induced deviations away from geodesic motion.

A more formal study of the MPD equations have also occurred in various forms [17–19], including a recent perturbative approach developed by Chicone, Mashhoon, and Punsly (CMP) [20], with application to the study of rotating plasma clumps propagating in astrophysical jets directed along a Kerr black hole's axis of symmetry. Another application of the CMP approximation by Mashhoon and Singh [21] determined analytic expressions for leading-order spin-curvature perturbations of a spinning particle's circular orbit around a Kerr black hole. This analysis is successful in reproducing the spinning particle's kinematic behavior compared to numerical simulations of the full MPD equations for situations where, for spin magnitude s and mass m, the Møller radius [21,22] for

*dinesh.singh@uregina.ca

the spinning particle is $s/m \lesssim 10^{-3}r$, and r is the particle's radial distance away from the background mass source. However, this approximation starts to break down when $s/(mr) \sim 10^{-2}$–10^{-1} for $r = 10M$, where M is the Kerr black hole mass, suggesting that higher-order spin-curvature coupling terms are required to more completely describe the orbital motion.

It was for this initial purpose that a generalization of the CMP approximation was very recently introduced by Singh [23] to incorporate higher-order analytic contributions to the perturbation approach for the MPD equations. This generalization has several nice features. For example, as a power series expansion with respect to the particle's spin magnitude, it can be extended to formally *infinite order* in the expansion. In addition, it leads to expressions that are background independent, and is fully applicable to *arbitrary motion* of the particle, without recourse to any space-time symmetries within the metric. As a result, this generalization is very robust, with applicability for many distinct scenarios in theoretical astrophysics, such as the modelling of globular clusters and other many-body dynamical systems in curved space-time, and also spinning particle interactions with gravitational waves, the results of which can be compared with existing treatments [24–26]. Furthermore, this approach identifies the existence of a classical analogue for ''radiative corrections'' that shift the particle's overall squared mass and spin magnitude due to higher-order spin-curvature contributions, a feature not thought about before. It would, therefore, be very useful to investigate the computational capacity of this generalization when applied to circular motion in the Kerr background. This is especially so in extreme conditions where a transition from stable to chaotic motion may be analytically identified, for comparison with existing approaches [11–14] which use primarily numerical methods.

The purpose of this paper is to present the generalized form of the CMP approximation for the MPD equations within the context of circular motion around a Kerr black hole, and explore the derived physical consequences. It begins with Sec. II, which displays the full MPD equations, followed by a presentation of the formalism behind the generalized CMP approximation in Sec. III. Afterwards, Sec. IV presents the formal application of the generalized CMP approximation to the case of circular motion around a Kerr black hole, up to second order in the perturbation expansion parameter. This is followed, in Sec. V, by analysis of the predicted kinematic and dynamical properties of the perturbed system, including the predicted effective squared mass and spin magnitude of the spinning particle. A general discussion of the main results obtained in this paper is found in Sec. VI, with a brief conclusion thereafter. The metric convention adopted is $+2$ signature with Riemann and Ricci tensor definitions following MTW [27], and geometric units of $G = c = 1$ are assumed throughout.

II. MATHISSON-PAPAPETROU-DIXON (MPD) EQUATIONS

The MPD equations of motion for the spinning particle's linear four-momentum $P^\mu(\tau)$ and spin tensor $S^{\alpha\beta}(\tau)$ consist of

$$\frac{DP^\mu}{d\tau} = -\frac{1}{2}R^\mu{}_{\nu\alpha\beta}u^\nu S^{\alpha\beta}, \tag{1a}$$

$$\frac{DS^{\alpha\beta}}{d\tau} = P^\alpha u^\beta - P^\beta u^\alpha, \tag{1b}$$

where (1a) describes the force applied due to spin-curvature coupling via $S^{\alpha\beta}(\tau)$, the particle's four-velocity vector $u^\mu(\tau) = dx^\mu(\tau)/d\tau$ with affine parametrization τ, and the Riemann curvature tensor $R_{\mu\nu\alpha\beta}$, while (1b) describes the corresponding torque generated. As a result of (1b), the particle's four-momentum precesses around the center-of-mass worldline. While it is possible to identify τ with proper time such that $u^\mu u_\mu = -1$, it is useful to leave it unspecified at present. The differences between competing descriptions of extended objects in curved space-time arise from differing higher-order multipole moment terms beyond the mass monopole and spin dipole moment, leading to additive contributions of the form $\mathcal{F}^\mu$ and $\mathcal{T}^{\alpha\beta}$ [17,21] in (1a) and (1b), respectively. Specification of $\mathcal{F}^\mu$ and $\mathcal{T}^{\alpha\beta}$ requires knowledge of the spinning object's energy-momentum tensor $T^{\mu\nu}$ [5–7,21], satisfying covariant conservation $T^{\mu\nu}{}_{;\nu} = 0$. For most practical purposes, however, the expression for (1) is sufficient.

At present, the MPD equations as expressed in (1) are underdetermined and require additional equations to completely specify the system. Following the approach from Dixon [5,6], the orthogonality spin condition relating the particle's linear and spin angular momenta according to

$$S^{\alpha\beta}P_\beta = 0 \tag{2}$$

is introduced, while the mass and spin parameters m and s naturally take the form

$$m^2 = -P_\mu P^\mu, \tag{3a}$$

$$s^2 = \tfrac{1}{2}S_{\mu\nu}S^{\mu\nu}. \tag{3b}$$

It is very important to note that, while (3a) and (3b) are both technically functions of τ, the MPD equations and (2) indicate that m and s are *constants of the motion* [20]. As well, the combination of (1) and (2) are known [9] to result in an expression for the four-velocity u^μ in terms of P^μ and $S^{\alpha\beta}$, such that

$$u^\mu = -\frac{P\cdot u}{m^2}\left[P^\mu + \frac{1}{2}\frac{S^{\mu\nu}R_{\nu\gamma\alpha\beta}P^\gamma S^{\alpha\beta}}{m^2 + \frac{1}{4}R_{\alpha\beta\rho\sigma}S^{\alpha\beta}S^{\rho\sigma}}\right], \tag{4}$$

where $P\cdot u$ is currently an undetermined scalar product relating the particle's internal clock with respect to τ. It becomes a self-evident confirmation from (4) that spin-curvature coupling displaces the particle's four-velocity

away from a geodesic in curved space-time, leading to a dynamically rich interplay between the particle's center-of-mass motion and its dynamical response due to spin-curvature interaction. The constraint equations (2)–(4) will prove very useful for ultimately deriving the generalized CMP approximation [23].

III. THE GENERALIZED CMP APPROXIMATION FOR THE MPD EQUATIONS

A. CMP approximation

The approach taken by Chicone, Mashhoon, and Punsly in deriving the CMP approximation [20,21] is to first assume that $P^\mu - mu^\mu = E^\mu$ is a small quantity, where E^μ is the spin-curvature force. As well, the Møller radius ρ [20–22] is chosen to be small, such that $\rho = s/m \ll r$, where r is the distance from the particle to the background gravitational source. This combination leads to the CMP approximation for the MPD equations, a series expansion to first order in s, such that

$$\frac{DP^\mu}{d\tau} \approx -\frac{1}{2}R^\mu{}_{\nu\alpha\beta}u^\nu S^{\alpha\beta}, \tag{5a}$$

$$\frac{DS^{\alpha\beta}}{d\tau} \approx 0, \tag{5b}$$

where the spin tensor in (5b) is parallel transported within the approximation, and the spin condition (2) takes the form

$$S^{\alpha\beta}u_\beta \approx 0, \tag{6}$$

coinciding with the Pirani condition [28] relating the orthogonality of the spin tensor to the four-velocity.

The CMP approximation is a useful first step in an analytic perturbation approach to the MPD equations, with a remarkably accurate description for circular motion around a Kerr black hole [21] compared to the full MPD equations for $s/(mr) \sim 10^{-3}$ and $r = 10M$. However, it becomes clear that the CMP approximation breaks down as $s/(mr) \sim 10^{-2}$–10^{-1} for the same choice of r, which follows from the loss of torque information due to (5b), especially since the spin-induced modulation of the particle's τ-dependent radial position found in the MPD equations is not present in the CMP approximation. This weakness within (5) and (6) is suggestive of a more detailed and systematic approach that has resulted in the generalization to follow [23].

B. Generalization of the CMP approximation

1. Formalism

The approach taken to generalize the CMP approximation is to assume a power series expansion of the particle's linear momentum and spin angular momentum, such that

$$P^\mu(\varepsilon) \equiv \sum_{j=0}^{\infty}\varepsilon^j P^\mu_{(j)}, \tag{7a}$$

$$S^{\mu\nu}(\varepsilon) \equiv \varepsilon\sum_{j=0}^{\infty}\varepsilon^j S^{\mu\nu}_{(j)} = \sum_{j=1}^{\infty}\varepsilon^j S^{\mu\nu}_{(j-1)}, \tag{7b}$$

where ε is an expansion parameter to be associated with s, and $P^\mu_{(j)}$ and $S^{\mu\nu}_{(j-1)}$ are the respective jth-order contributions of the linear momentum and spin angular momentum in ε. This implies that the zeroth-order expressions in ε denote the dynamics of a spinless particle in geodesic motion. As well, the four-velocity is assumed to take the form

$$u^\mu(\varepsilon) \equiv \sum_{j=0}^{\infty}\varepsilon^j u^\mu_{(j)}. \tag{8}$$

When substituting (7) and (8) into the MPD equations described by

$$\frac{DP^\mu(\varepsilon)}{d\tau} = -\frac{1}{2}R^\mu{}_{\nu\alpha\beta}u^\nu(\varepsilon)S^{\alpha\beta}(\varepsilon), \tag{9a}$$

$$\frac{DS^{\alpha\beta}(\varepsilon)}{d\tau} = 2\varepsilon P^{[\alpha}(\varepsilon)u^{\beta]}(\varepsilon), \tag{9b}$$

where an extra factor of ε is introduced in (9b) for consistency, it follows that the jth-order expressions of the MPD equations are

$$\frac{DP^\mu_{(j)}}{d\tau} = -\frac{1}{2}R^\mu{}_{\nu\alpha\beta}\sum_{k=0}^{j-1}u^\nu_{(j-1-k)}S^{\alpha\beta}_{(k)}, \tag{10a}$$

$$\frac{DS^{\alpha\beta}_{(j-1)}}{d\tau} = 2\sum_{k=0}^{j-1}P^{[\alpha}_{(j-1-k)}u^{\beta]}_{(k)}. \tag{10b}$$

Given $P^\mu_{(0)} = m_0 u^\mu_{(0)}$, where

$$m_0^2 \equiv -P^{(0)}_\mu P^\mu_{(0)}, \tag{11}$$

it can be shown that the zeroth-order term in ε is

$$\frac{DP^\mu_{(0)}}{d\tau} = 0, \tag{12}$$

while the respective first-order terms following (10) are

$$\frac{DP^\mu_{(1)}}{d\tau} = -\frac{1}{2}R^\mu{}_{\nu\alpha\beta}u^\nu_{(0)}S^{\alpha\beta}_{(0)}, \tag{13a}$$

$$\frac{DS^{\alpha\beta}_{(0)}}{d\tau} = 0, \tag{13b}$$

which is the CMP approximation.

2. Supplementary equations

A complete specification of (10) requires determining $u^\mu_{(j)}$ as a function of the linear and spin angular momentum expansion components. In turn, this requires use of the supplementary equations (2)–(4), which have important

consequences within the formalism. It is straightforward to show that the spin condition (2) in terms of (7a) and (7b) is

$$P^{(0)}_{\mu} S^{\mu\nu}_{(j)} = -\sum_{k=1}^{j} P^{(k)}_{\mu} S^{\mu\nu}_{(j-k)}, \qquad j \geq 1 \tag{14}$$

for the $(j+1)$th-order contribution in ε, where the first-order perturbation in ε is

$$P^{(0)}_{\mu} S^{\mu\nu}_{(0)} = 0. \tag{15}$$

Given that the mass and spin magnitude parameters m and s described by (3) are dependent on P^{μ} and $S^{\mu\nu}$, which are represented by (7a) and (7b), respectively, it is possible to identify a classical analogue of a *bare mass* m_0 defined by (11) and a *bare spin* s_0, according to

$$s_0^2 \equiv \tfrac{1}{2} S^{(0)}_{\mu\nu} S^{\mu\nu}_{(0)}, \tag{16}$$

in analogy with the radiative corrections identified with the bare mass and spin parameters in quantum field theory. In this way, the MPD equations in perturbative form yield total mass and spin magnitudes due to the sum of "radiative corrections" to m_0 and s_0, such that

$$m^2(\varepsilon) = m_0^2\left(1 + \sum_{j=1}^{\infty} \varepsilon^j \bar{m}_j^2\right), \tag{17}$$

$$s^2(\varepsilon) = \varepsilon^2 s_0^2\left(1 + \sum_{j=1}^{\infty} \varepsilon^j \bar{s}_j^2\right), \tag{18}$$

where

$$\bar{m}_j^2 = -\frac{1}{m_0^2} \sum_{k=0}^{j} P^{(j-k)}_{\mu} P^{\mu}_{(k)}, \tag{19}$$

$$\bar{s}_j^2 = \frac{1}{s_0^2} \sum_{k=0}^{j} S^{(j-k)}_{\mu\nu} S^{\mu\nu}_{(k)}, \tag{20}$$

are dimensionless jth-order corrections to m_0^2 and s_0^2, respectively. Given that m^2 and s^2 are already shown to be constant within the exact set of MPD equations, it must also be true that $\bar{m}_j^2$ and $\bar{s}_j^2$ are individually constant for each order of ε.

For the remaining supplementary equation (4), the four-velocity described by

$$u^{\mu}(\varepsilon) = -\frac{P\cdot u}{m^2(\varepsilon)}\left[P^{\mu}(\varepsilon) + \frac{1}{2}\frac{S^{\mu\nu}(\varepsilon) R_{\nu\gamma\alpha\beta} P^{\gamma}(\varepsilon) S^{\alpha\beta}(\varepsilon)}{m^2(\varepsilon)\Delta(\varepsilon)}\right], \tag{21a}$$

$$\Delta(\varepsilon) \equiv 1 + \frac{1}{4m^2(\varepsilon)} R_{\mu\nu\alpha\beta} S^{\mu\nu}(\varepsilon) S^{\alpha\beta}(\varepsilon), \tag{21b}$$

can be determined as a series expansion in ε, upon specifying the yet undetermined scalar product $P\cdot u$. With the particularly useful choice of

$$P\cdot u \equiv -m(\varepsilon), \tag{22}$$

it is straightforward to determine that

$$\begin{aligned} u_{\mu}(\varepsilon) u^{\mu}(\varepsilon) &= -1 + \frac{1}{4m^6(\varepsilon)\Delta^2(\varepsilon)} \tilde{R}_{\mu}(\varepsilon)\tilde{R}^{\mu}(\varepsilon) \\ &= -1 + O(\varepsilon^4), \end{aligned} \tag{23}$$

where

$$\tilde{R}^{\mu}(\varepsilon) \equiv S^{\mu\nu}(\varepsilon) R_{\nu\gamma\alpha\beta} P^{\gamma}(\varepsilon) S^{\alpha\beta}(\varepsilon). \tag{24}$$

To at least third order in ε, the outcome (23) from (22) justifies the identification of τ as *proper time* for parametrization of the particle's center-of-mass worldline. It is also straightforward, though tedious, to show explicitly from substituting (7) and (17) into (21) that the spinning particle's four-velocity in general form is

$$\begin{aligned} u^{\mu}(\varepsilon) &= \sum_{j=0}^{\infty} \varepsilon^j u^{\mu}_{(j)} \\ &= \frac{P^{\mu}_{(0)}}{m_0} + \varepsilon\left[\frac{1}{m_0}\left(P^{\mu}_{(1)} - \frac{1}{2}\bar{m}_1^2 P^{\mu}_{(0)}\right)\right] + \varepsilon^2\left\{\frac{1}{m_0}\left[P^{\mu}_{(2)} - \frac{1}{2}\bar{m}_1^2 P^{\mu}_{(1)} - \frac{1}{2}\left(\bar{m}_2^2 - \frac{3}{4}\bar{m}_1^4\right)P^{\mu}_{(0)}\right] + \frac{1}{2m_0^3} S^{\mu\nu}_{(0)} R_{\nu\gamma\alpha\beta} P_{(0)\gamma} S^{\alpha\beta}_{(0)}\right\} \\ &\quad + \varepsilon^3\left\{\frac{1}{m_0}\left[P^{\mu}_{(3)} - \frac{1}{2}\bar{m}_1^2 P^{\mu}_{(2)} - \frac{1}{2}\left(\bar{m}_2^2 - \frac{3}{4}\bar{m}_1^4\right)P^{\mu}_{(1)} - \frac{1}{2}\left(\bar{m}_3^2 - \frac{3}{2}\bar{m}_1^2\bar{m}_2^2 + \frac{5}{8}\bar{m}_1^6\right)P^{\mu}_{(0)}\right]\right. \\ &\quad \left. + \frac{1}{2m_0^3} R_{\nu\gamma\alpha\beta}\left[\sum_{n=0}^{1} S^{\mu\nu}_{(1-n)} \sum_{k=0}^{n} P^{\gamma}_{(n-k)} S^{\alpha\beta}_{(k)} - \frac{3}{2}\bar{m}_1^2 S^{\mu\nu}_{(0)} P^{\gamma}_{(0)} S^{\alpha\beta}_{(0)}\right]\right\} + O(\varepsilon^4), \end{aligned} \tag{25}$$

which also satisfies (23) to third order in ε. Following (25), it can be verified that [23]

$$\frac{D\bar{s}_j^2}{d\tau} = \frac{D\bar{m}_j^2}{d\tau} = 0 \tag{26}$$

up to third order in ε, with the use of (10).

3. Perturbations of the Møller radius

A useful consideration within the generalized CMP approximation is the perturbation expression for the Møller radius $\rho = s/m$, since this quantity is relevant for identifying the strength of the spin-curvature interaction for particles in the Kerr background while in circular orbit [21]. From previous work on chaotic dynamics [11–14], there is a strong suggestion that perturbations in the Møller radius may give some insight into determining the precise conditions for a transition away from stable motion. A straightforward calculation shows that

$$\frac{s(\varepsilon)}{m(\varepsilon)} = \varepsilon\frac{s_0}{m_0}\Big\{1 + \varepsilon\Big[\frac{1}{2}(\bar{s}_1^2 - \bar{m}_1^2)\Big] + \varepsilon^2\Big[\frac{1}{2}(\bar{s}_2^2 - \bar{m}_2^2) - \frac{1}{4}\bar{s}_1^2\bar{m}_1^2 - \frac{1}{8}(\bar{s}_1^4 - 3\bar{m}_1^4)\Big] + O(\varepsilon^3)\Big\}, \tag{27}$$

where the second- and third-order contributions in ε due to the "radiative corrections" formally shift the perturbed terms away from $\rho_0 = s_0/m_0$. However, the precise nature of the shift from ρ_0 to ρ requires determining (27) in terms of a specific background.

C. Solving for linear momentum and spin angular momentum expansion components

1. Local Fermi coordinate frame

Having now presented the generalized CMP approximation, the next step is to determine the linear momentum and spin angular momentum series expansion components for (7). This can be accomplished iteratively by solving the first-order perturbations with respect to zeroth-order quantities, and then computing the higher-order terms in a systematic fashion. This approach becomes particularly straightforward upon framing the problem in terms of the tetrad formalism and Fermi normal coordinates [21], the latter of which has the property that the corresponding metric in the neighborhood of a freely falling worldline is locally flat. The leading-order metric deviations in Fermi normal coordinates are then proportional to the projected Riemann curvature tensor in the Fermi frame evaluated on the worldline.

To begin, consider an orthonormal tetrad frame $\lambda^{\mu}{}_{\hat{\alpha}}$ with the orthogonality condition

$$\eta_{\hat{\alpha}\hat{\beta}} = g_{\mu\nu}\lambda^{\mu}{}_{\hat{\alpha}}\lambda^{\nu}{}_{\hat{\beta}} \tag{28}$$

satisfying parallel transport

$$\frac{D\lambda^{\mu}{}_{\hat{\alpha}}}{d\tau} = 0 \tag{29}$$

with respect to the general space-time coordinates X^{μ}, where $\hat{\alpha}$ are indices for the Fermi coordinates $X^{\hat{\alpha}}$ defined in the neighborhood of the spinning particle on a locally flat tangent space. Furthermore, the Riemann curvature tensor in the Fermi frame is described by

$${}^{F}R_{\hat{\alpha}\hat{\beta}\hat{\gamma}\hat{\delta}} = R_{\mu\nu\rho\sigma}\lambda^{\mu}{}_{\hat{\alpha}}\lambda^{\nu}{}_{\hat{\beta}}\lambda^{\rho}{}_{\hat{\gamma}}\lambda^{\sigma}{}_{\hat{\delta}}. \tag{30}$$

By identifying $\lambda^{\mu}{}_{\hat{0}} = u^{\mu}_{(0)}$ in the usual fashion and making use of (28) and the first-order spin condition, it follows naturally that

$$P^{\mu}_{(0)} = \lambda^{\mu}{}_{\hat{\alpha}}P^{\hat{\alpha}}_{(0)} = m_0\lambda^{\mu}{}_{\hat{0}}, \tag{31a}$$

$$S^{\mu\nu}_{(0)} = \lambda^{\mu}{}_{\hat{\imath}}\lambda^{\nu}{}_{\hat{\jmath}}S^{\hat{\imath}\hat{\jmath}}_{(0)}, \tag{31b}$$

where $P^{\hat{\alpha}}_{(0)} = m_0\delta^{\hat{\alpha}}{}_{\hat{0}}$ and $S^{\hat{\imath}\hat{\jmath}}_{(0)}$ is a constant-valued spatial antisymmetric tensor whose components are determined from initial conditions.

2. Leading perturbation of linear momentum and spin angular momentum

Determining the first-order perturbation in ε for the linear momentum is very straightforward. Given (13a) and (29), it is shown that $DP^{\mu}_{(1)}/d\tau = \lambda^{\mu}{}_{\hat{\alpha}}(dP^{\hat{\alpha}}_{(1)}/d\tau)$, leading to

$$\frac{dP^{\hat{\alpha}}_{(1)}}{d\tau} = -\frac{1}{2}{}^{F}R^{\hat{\alpha}}{}_{\hat{0}\hat{\imath}\hat{\jmath}}S^{\hat{\imath}\hat{\jmath}}_{(0)}, \tag{32}$$

which can be integrated immediately with the final result of

$$P^{\mu}_{(1)} = -\frac{1}{2}\lambda^{\mu}{}_{\hat{k}}\int({}^{F}R^{\hat{k}}{}_{\hat{0}\hat{\imath}\hat{\jmath}}S^{\hat{\imath}\hat{\jmath}}_{(0)})d\tau. \tag{33}$$

It is interesting to note that, when (33) is contracted with $P^{(0)}_{\mu}$, the first-order mass shift contribution is identically

$$\bar{m}_1^2 = 0 \tag{34}$$

for a general space-time background, leading to simplified expressions for (25) and (27).

The corresponding expression for the spin tensor, in contrast to the linear momentum, is somewhat more complicated to determine. It is important to first note that, from (10b) for $j = 2$,

$$\frac{DS^{\mu\nu}_{(1)}}{d\tau} = 0. \tag{35}$$

In terms of the tetrad projection,

$$S^{\mu\nu}_{(1)} = \lambda^{\mu}{}_{\hat{\alpha}}\lambda^{\nu}{}_{\hat{\beta}}S^{\hat{\alpha}\hat{\beta}}_{(1)} = 2\lambda^{[\mu}{}_{\hat{0}}\lambda^{\nu]}{}_{\hat{\jmath}}S^{\hat{0}\hat{\jmath}}_{(1)} + \lambda^{\mu}{}_{\hat{\imath}}\lambda^{\nu}{}_{\hat{\jmath}}S^{\hat{\imath}\hat{\jmath}}_{(1)}, \tag{36}$$

where it follows from (14) for $j = 1$ that

$$S^{\hat{0}\hat{\jmath}}_{(1)} = -\frac{1}{m_0}P^{(1)}_{\hat{\imath}}S^{\hat{\imath}\hat{\jmath}}_{(0)}. \tag{37}$$

As for the components $S^{\hat{\imath}\hat{\jmath}}_{(1)}$ in (36), they can be formally determined from using (20) for $j = 1$, such that

$$S^{\hat{\imath}\hat{\jmath}}_{(1)} = \tfrac{1}{4}\bar{s}_1^2S^{\hat{\imath}\hat{\jmath}}_{(0)}. \tag{38}$$

This, however, leads to a difficulty, in that (36) is still dependent on a yet *undetermined parameter* $\bar{s}_1^2$. While it is tempting to set $\bar{s}_1^2 = 0$ in analogy with $\bar{m}_1^2 = 0$, this is not well justified considering that $\bar{s}_1^2$ only needs to be *covariantly constant* following (26), and not necessarily zero.

Fortunately, $\bar{s}_1^2$ can be determined separately by directly solving (35), following a variation of an approach presented earlier [23]. Making use of the spin condition constraint equation with (14) for $j = 1$, there exist four equations

$$A^\mu S^{(1)}_{\mu\nu} - B_\nu = 0, \tag{39}$$

where

$$A^\mu \equiv P^\mu_{(0)}, \tag{40a}$$

$$B_\nu \equiv -P^\mu_{(1)} S^{(0)}_{\mu\nu}. \tag{40b}$$

With (39), it is possible to algebraically solve for the $S^{(1)}_{0j}$ components in terms of the purely spatial components $S^{(1)}_{ij}$, such that

$$S^{(1)}_{01} = \frac{1}{A^0}[A^2 S^{(1)}_{12} - A^3 S^{(1)}_{31} + B_1], \tag{41a}$$

$$S^{(1)}_{02} = \frac{1}{A^0}[A^3 S^{(1)}_{23} - A^1 S^{(1)}_{12} + B_2], \tag{41b}$$

$$S^{(1)}_{03} = \frac{1}{A^0}[A^1 S^{(1)}_{31} - A^2 S^{(1)}_{23} + B_3]. \tag{41c}$$

The remaining three components can then be determined by solving (35) in covariant form for the spatial components, leading to

$$\frac{DS^{(1)}_{ij}}{d\tau} = \frac{dS^{(1)}_{ij}}{d\tau} + 2u^\alpha_{(0)} \Gamma^\beta{}_{\alpha[i} S^{(1)}_{j]\beta} = 0. \tag{42}$$

Upon substituting (41) into (42), there now exists a first-order inhomogeneous matrix differential equation to solve, with components

$$\frac{dS^{(1)}_{12}(\tau)}{d\tau} + \frac{1}{2}\alpha^{ij} S^{(1)}_{ij}(\tau) = \delta_{12}(\tau), \tag{43a}$$

$$\frac{dS^{(1)}_{23}(\tau)}{d\tau} + \frac{1}{2}\beta^{ij} S^{(1)}_{ij}(\tau) = \delta_{23}(\tau), \tag{43b}$$

$$\frac{dS^{(1)}_{31}(\tau)}{d\tau} + \frac{1}{2}\gamma^{ij} S^{(1)}_{ij}(\tau) = \delta_{31}(\tau), \tag{43c}$$

where the antisymmetric spatial tensors α^{ij}, β^{ij}, and γ^{ij} may each be τ dependent, depending on the choice of metric, and the $\delta_{ij}(\tau)$ are due to (40b).

3. Higher-order perturbation terms

Proceeding beyond the leading-order perturbations of P^μ and $S^{\alpha\beta}$ is very straightforward. For the linear momentum, the second-order expression is

$$\begin{aligned} P^\mu_{(2)} &= -\frac{1}{2}\lambda^\mu{}_{\hat{\alpha}} \int \left(\frac{1}{m_0} {}^F R^{\hat{\alpha}}{}_{\hat{\beta}\hat{k}\hat{l}} P^{\hat{\beta}}_{(1)} S^{\hat{k}\hat{l}}_{(0)} + {}^F R^{\hat{\alpha}}{}_{\hat{0}\hat{\gamma}\hat{\beta}} S^{\hat{\gamma}\hat{\beta}}_{(1)} \right) d\tau \\ &\approx -\frac{1}{2}\lambda^\mu{}_{\hat{\alpha}} \int \left(\frac{1}{m_0} {}^F R^{\hat{\alpha}}{}_{\hat{\beta}\hat{k}\hat{l}} P^{\hat{\beta}}_{(1)} + \frac{1}{4}\langle \bar{s}_1^2 \rangle {}^F R^{\hat{\alpha}}{}_{\hat{0}\hat{k}\hat{l}} \right. \\ &\quad \left. - \frac{2}{m_0} {}^F R^{\hat{\alpha}}{}_{\hat{0}\hat{0}\hat{l}} P^{(1)}_{\hat{k}} \right) S^{\hat{k}\hat{l}}_{(0)} d\tau, \end{aligned} \tag{44}$$

where

$$\langle \bar{s}_j^2 \rangle = \frac{1}{T}\int_0^T \bar{s}_j^2(\tau) d\tau \tag{45}$$

is the time-averaged jth-order correction to the squared spin magnitude. To determine the second-order spin tensor, it is first shown from (10b) for $j = 3$ that

$$\frac{DS^{\mu\nu}_{(2)}}{d\tau} = \frac{1}{m_0^3} P^{[\mu}_{(0)} S^{\nu]\sigma}_{(0)} R_{\sigma\gamma\alpha\beta} P^\gamma_{(0)} S^{\alpha\beta}_{(0)}. \tag{46}$$

When expressed in terms of the orthonormal tetrad, it follows that (46) can be solved easily to obtain

$$S^{\mu\nu}_{(2)} = \frac{1}{m_0}\lambda^{[\mu}{}_{\hat{0}} \lambda^{\nu]}{}_{\hat{\imath}} \int S^{\hat{\imath}\hat{\jmath}}_{(0)} {}^F R_{\hat{\jmath}\hat{0}\hat{k}\hat{l}} S^{\hat{k}\hat{l}}_{(0)} d\tau. \tag{47}$$

IV. CIRCULAR MOTION NEAR THE EVENT HORIZON OF A KERR BLACK HOLE

With the generalized CMP approximation of the MPD equations established, it can now be applied to the concrete example of a spinning particle in circular motion around a Kerr black hole in the equatorial plane near its event horizon. It would be interesting to identify the general interplay between black hole spin and the dynamical response from the spinning particle. Since it is known that an orbiting particle whose spin corotates with the black hole spin leads to a repulsive force, while one of opposite spin to the black hole leads to an attractive force [20], it is particularly useful to determine the black hole's spin dependence on the kinematics and dynamics of the particle's orbit due to contributions beyond the CMP approximation considered earlier [21].

To begin, consider a Kerr background in standard Boyer-Lindquist coordinates $X^\mu = (t, r, \theta, \phi)$, described in terms of a black hole mass M and specific spin angular momentum $a = J/M$. Then, for constant radius r, the solution to the geodesic equation for circular motion is [21]

$$t = \frac{1}{N}(1 + a\Omega_{\mathrm{K}})\tau, \tag{48a}$$

$$\phi = \frac{\Omega_{\mathrm{K}}\tau}{N \sin\theta}, \tag{48b}$$

where $\theta = \pi/2$ on the equatorial plane,

$$\Omega_{\mathrm{K}} = \sqrt{\frac{M}{r^3}} \tag{49}$$

is the Keplerian frequency of the orbit and

$$N = \sqrt{1 - \frac{3M}{r} + 2a\Omega_{\rm K}} \tag{50}$$

is a normalization constant. At $\tau = 0$, the boundary conditions are chosen such that $t = \phi = 0$. Given that $\lambda^{\mu}{}_{\hat{0}} = dX^{\mu}/d\tau$ is the particle's four-velocity vector, and that the orthonormal tetrad frame satisfies $D\lambda^{\mu}{}_{\hat{\alpha}}/d\tau = 0$, it is possible to determine unit gyro axes $\lambda^{\mu}{}_{\hat{\imath}}$ to describe the particle's local spatial frame. It is straightforward to show that [21,29]

$$\lambda^{\mu}{}_{\hat{0}} = \left(\frac{1 + a\Omega_{\rm K}}{N}, 0, 0, \frac{\Omega_{\rm K}}{N\sin\theta}\right), \tag{51a}$$

$$\lambda^{\mu}{}_{\hat{1}} = \left(-\frac{L}{rA}\sin(\Omega_{\rm K}\tau), A\cos(\Omega_{\rm K}\tau), 0, -\frac{E}{rA\sin\theta}\sin(\Omega_{\rm K}\tau)\right), \tag{51b}$$

$$\lambda^{\mu}{}_{\hat{2}} = \left(0, 0, \frac{1}{r}, 0\right), \tag{51c}$$

$$\lambda^{\mu}{}_{\hat{3}} = \left(\frac{L}{rA}\cos(\Omega_{\rm K}\tau), A\sin(\Omega_{\rm K}\tau), 0, \frac{E}{rA\sin\theta}\cos(\Omega_{\rm K}\tau)\right), \tag{51d}$$

where

$$E = \frac{1}{N}\left(1 - \frac{2M}{r} + a\Omega_{\rm K}\right), \tag{52a}$$

$$L = \frac{r^2\Omega_{\rm K}}{N}\left(1 - 2a\Omega_{\rm K} + \frac{a^2}{r^2}\right), \tag{52b}$$

$$A = \sqrt{1 - \frac{2M}{r} + \frac{a^2}{r^2}}, \tag{52c}$$

for the circular orbit's energy E and orbital angular momentum L. It is useful to describe a by the dimensionless parameter $\alpha = a/r$, such that $-1/4 \le \alpha \le 1$ to incorporate black hole spin ($-M \le a \le M$) that is both corotating and counterrotating with respect to the orbital direction, where $r_{0+} = M$ for $\alpha = 1$ and $r_{0-} = 4M$ for $\alpha = -1/4$, each corresponding to the innermost (photon) radius allowed [30]. All dimensional quantities are then described with respect to M, such that

$$r = 9M\left[\alpha + \sqrt{\alpha^2 + 3(1 - N^2)}\right]^{-2} \tag{53}$$

is the orbital radius near the event horizon and $N \gtrsim 0$ denotes the separation away from the innermost circular orbit. The parameters (52) are now expressible in terms of

$$E_0 = 1 - 2(r^2\Omega_{\rm K}^2) + \alpha(r\Omega_{\rm K}) = NE, \tag{54a}$$

$$L_0 = (r\Omega_{\rm K})[1 - 2\alpha(r\Omega_{\rm K}) + \alpha^2] = N\frac{L}{r}, \tag{54b}$$

where $\Delta = r^2[1 - 2(r^2\Omega_{\rm K}^2) + \alpha^2] = r^2A^2$ is the known function defined in the Kerr metric [30].

The exact expressions for ${}^{F}R_{\hat{\mu}\hat{\nu}\hat{\alpha}\hat{\beta}}$ are listed in Appendix A. For the special case of $N \to 0$ and $\theta = \pi/2$ considered in this paper, the dominant nonzero contributions of the Riemann curvature tensor ${}^{F}R_{\hat{\mu}\hat{\nu}\hat{\alpha}\hat{\beta}}$ in the Fermi frame are

$${}^{F}R_{\hat{0}\hat{1}\hat{0}\hat{1}} \approx -\frac{\Omega_{\rm K}^2}{N^2}[2A^2 + r^2\Omega_{\rm K}^2 - \alpha(2r\Omega_{\rm K} - \alpha)] \times \cos^2(\Omega_{\rm K}\tau) = -{}^{F}R_{\hat{2}\hat{3}\hat{2}\hat{3}}, \tag{55a}$$

$${}^{F}R_{\hat{0}\hat{1}\hat{0}\hat{3}} \approx -\frac{\Omega_{\rm K}^2}{N^2}[2A^2 + r^2\Omega_{\rm K}^2 - \alpha(2r\Omega_{\rm K} - \alpha)] \times \sin(\Omega_{\rm K}\tau)\cos(\Omega_{\rm K}\tau) = -{}^{F}R_{\hat{1}\hat{2}\hat{2}\hat{3}}, \tag{55b}$$

$${}^{F}R_{\hat{0}\hat{1}\hat{1}\hat{3}} \approx \frac{3\Omega_{\rm K}^2A}{N^2}(r\Omega_{\rm K} - \alpha)\cos(\Omega_{\rm K}\tau) = -{}^{F}R_{\hat{0}\hat{2}\hat{2}\hat{3}}, \tag{55c}$$

$${}^{F}R_{\hat{0}\hat{2}\hat{0}\hat{2}} \approx \frac{\Omega_{\rm K}^2}{N^2}[1 - 2\alpha(2r\Omega_{\rm K} - \alpha)] = -{}^{F}R_{\hat{1}\hat{3}\hat{1}\hat{3}}, \tag{55d}$$

$${}^{F}R_{\hat{0}\hat{2}\hat{1}\hat{2}} \approx -\frac{3\Omega_{\rm K}^2A}{N^2}(r\Omega_{\rm K} - \alpha)\sin(\Omega_{\rm K}\tau) = -{}^{F}R_{\hat{0}\hat{3}\hat{1}\hat{3}}, \tag{55e}$$

$${}^{F}R_{\hat{0}\hat{3}\hat{0}\hat{3}} \approx -\frac{\Omega_{\rm K}^2}{N^2}[2A^2 + r^2\Omega_{\rm K}^2 - \alpha(2r\Omega_{\rm K} - \alpha)] \times \sin^2(\Omega_{\rm K}\tau) = -{}^{F}R_{\hat{1}\hat{2}\hat{1}\hat{2}}. \tag{55f}$$

A. First-order perturbations in ε

With all the ground work for the application of the generalized CMP approximation now complete, it is possible to begin computing the linear and higher-order perturbations of the linear momentum and spin tensor for a spinning point particle in circular orbit. In this context, the expansion parameter ε is associated with the unperturbed Møller radius $\rho_0 = s_0/m_0$ in unit of r, such that $s_0/(m_0 r) \ll 1$.

To begin, recall from (31a) that (51a) that the unperturbed four-momentum components are

$$P^0_{(0)} = \frac{m_0}{N}(1 + \alpha r\Omega_{\rm K}), \tag{56a}$$

$$P^1_{(0)} = 0, \tag{56b}$$

$$P^2_{(0)} = 0, \tag{56c}$$

$$P^3_{(0)} = \frac{m_0}{N}\Omega_{\rm K}. \tag{56d}$$

Obtaining the first-order perturbation (CMP approximation) is very straightforward. Given (31b) and noting that the spinning particle is initially located on the x-axis of the Cartesian frame, the initial spin orientation $(\hat{\theta}, \hat{\phi})$ for $S^{\mu\nu}_{(0)}$ coincides with the standard definition for the spherical coordinates (θ, ϕ) with respect to the Cartesian frame's z-axis. Therefore, it follows that the projected spin tensor

components are [21]

$$S^{\hat{2}\hat{3}}_{(0)} = s_0 \sin\hat{\theta}\cos\hat{\phi}, \tag{57a}$$

$$S^{\hat{3}\hat{1}}_{(0)} = -s_0 \cos\hat{\theta}, \tag{57b}$$

$$S^{\hat{1}\hat{2}}_{(0)} = s_0 \sin\hat{\theta}\sin\hat{\phi}, \tag{57c}$$

leading to

$$S^{01}_{(0)}(\tau) = -\frac{m_0 r L_0}{N}\left(\frac{s_0}{m_0 r}\right)\cos\hat{\theta}, \tag{58a}$$

$$S^{02}_{(0)}(\tau) = -\frac{1}{2}\frac{m_0 L_0}{NA}\left(\frac{s_0}{m_0 r}\right)[\sin(\Omega_{\rm K}\tau + \hat{\theta} - \hat{\phi}) - \sin(\Omega_{\rm K}\tau - \hat{\theta} - \hat{\phi})], \tag{58b}$$

$$S^{03}_{(0)}(\tau) = 0, \tag{58c}$$

$$S^{12}_{(0)}(\tau) = \frac{1}{2} m_0 A\left(\frac{s_0}{m_0 r}\right)[\cos(\Omega_{\rm K}\tau + \hat{\theta} - \hat{\phi}) - \cos(\Omega_{\rm K}\tau - \hat{\theta} - \hat{\phi})], \tag{58d}$$

$$S^{23}_{(0)}(\tau) = \frac{1}{2}\frac{m_0 E_0}{rNA}\left(\frac{s_0}{m_0 r}\right)[\sin(\Omega_{\rm K}\tau + \hat{\theta} - \hat{\phi}) - \sin(\Omega_{\rm K}\tau - \hat{\theta} - \hat{\phi})], \tag{58e}$$

$$S^{31}_{(0)}(\tau) = -\frac{m_0 E_0}{N}\left(\frac{s_0}{m_0 r}\right)\cos\hat{\theta}. \tag{58f}$$

It is interesting to note the appearance of a beat structure in the sinusoidal functions of (58), due to the initial spin orientation angles. As for the first-order perturbation for the linear momentum, this follows naturally from (33), resulting in

$$P^0_{(1)}(\tau) = \frac{3}{2}\frac{m_0 L_0}{N^3}\left(\frac{s_0}{m_0 r}\right)(r\Omega_{\rm K})(r\Omega_{\rm K} - \alpha) \times [\cos(\Omega_{\rm K}\tau + \hat{\theta}) + \cos(\Omega_{\rm K}\tau - \hat{\theta}) - 2\cos\hat{\theta}], \tag{59a}$$

$$P^1_{(1)}(\tau) = \frac{3}{2}\frac{m_0 A^2}{N^2}\left(\frac{s_0}{m_0 r}\right)(r\Omega_{\rm K})(r\Omega_{\rm K} - \alpha) \times [\sin(\Omega_{\rm K}\tau + \hat{\theta}) + \sin(\Omega_{\rm K}\tau - \hat{\theta})], \tag{59b}$$

$$P^2_{(1)}(\tau) = \frac{3}{2}\frac{m_0 A}{rN^2}\left(\frac{s_0}{m_0 r}\right)(r\Omega_{\rm K})(r\Omega_{\rm K} - \alpha) \times [\cos(\Omega_{\rm K}\tau + \hat{\theta} - \hat{\phi}) - \cos(\Omega_{\rm K}\tau - \hat{\theta} - \hat{\phi}) + \cos(\hat{\theta} + \hat{\phi}) - \cos(\hat{\theta} - \hat{\phi})], \tag{59c}$$

$$P^3_{(1)}(\tau) = \frac{3}{2}\frac{m_0 E_0}{rN^3}\left(\frac{s_0}{m_0 r}\right)(r\Omega_{\rm K})(r\Omega_{\rm K} - \alpha) \times [\cos(\Omega_{\rm K}\tau + \hat{\theta}) + \cos(\Omega_{\rm K}\tau - \hat{\theta}) - 2\cos\hat{\theta}], \tag{59d}$$

which also exhibits a beat structure similar to what is found in (58). It is also interesting to note the relationship between the azimuthal and time component of $P^\mu_{(1)}$ in the form

$$\frac{P^3_{(1)}(\tau)}{P^0_{(1)}(\tau)} = \frac{E}{L}, \tag{60}$$

in agreement with the same computation performed earlier [21]. At this point, it is important to understand the conditions for the collapse of (59) when $(r\Omega_{\rm K} - \alpha) = 0$. This condition can appear when

$$r_{\rm c} = \left(\frac{a}{M}\right)^2 M, \tag{61}$$

which is theoretically possible to reach when $a = M$ [30]. However, it seems unlikely that such a possibility would arise in a realistic astrophysical context.

B. Higher-order perturbations in ε

Evaluation of the second-order perturbation quantities is also straightforward, though rather involved. There are, however, relatively compact expressions for higher-order perturbation quantities in ε that are required to evaluate the perturbed Møller radius (27), namely, the "radiative corrections" to the squared mass and spin magnitudes (19) and (20). The first computation of interest is $\bar{s}^2_1$, which is third order in ε according to (18). This is achieved by solving the first-order inhomogeneous matrix differential equation (43) for $S^{(1)}_{ij}(\tau)$, followed by the algebraic equation (41) for the remaining components $S^{(1)}_{0j}(\tau)$, which yields $\bar{s}^2_1$ via (20). Before proceeding, it is useful to first introduce a convenient notation for beat functions taking the form

$$Q^{\pm}_{\rm c}(n_1\Omega_{\rm K}\tau, n_2\hat{\theta}, n_3\hat{\phi}) \equiv \cos(n_1\Omega_{\rm K}\tau + n_2\hat{\theta} - n_3\hat{\phi}) \pm \cos(n_1\Omega_{\rm K}\tau - n_2\hat{\theta} - n_3\hat{\phi}), \tag{62a}$$

$$Q^{\pm}_{\rm s}(n_1\Omega_{\rm K}\tau, n_2\hat{\theta}, n_3\hat{\phi}) \equiv \sin(n_1\Omega_{\rm K}\tau + n_2\hat{\theta} - n_3\hat{\phi}) \pm \sin(n_1\Omega_{\rm K}\tau - n_2\hat{\theta} - n_3\hat{\phi}), \tag{62b}$$

which appear frequently in subsequent expressions throughout this paper. For the Kerr metric, it is shown that the nonzero α^{ij}, β^{ij}, and γ^{ij} for (43) are

$$\alpha^{23} = \frac{N}{rA^2}\frac{\Omega_{\rm K}}{(1 + \alpha r\Omega_{\rm K})}, \tag{63a}$$

$$\beta^{12} = -\frac{A^2}{N}(r\Omega_{\rm K})(1 + \alpha r\Omega_{\rm K}), \tag{63b}$$

while

$$\delta_{12}(\tau) = -\frac{3}{4}\frac{m_0 r L_0}{N^2 A}\left(\frac{s_0}{m_0 r}\right)^2 \frac{(r^2\Omega_{\rm K}^2)(r\Omega_{\rm K}-\alpha)}{(1+\alpha r\Omega_{\rm K})} Q_{\rm s}^{-}(\Omega_{\rm K}\tau, 2\hat{\theta}, \hat{\phi}), \tag{64a}$$

$$\delta_{23}(\tau) = 0, \tag{64b}$$

$$\delta_{31}(\tau) = \frac{3}{8}\frac{m_0 r L_0}{N^3}\left(\frac{s_0}{m_0 r}\right)^2 (r^2\Omega_{\rm K}^2)(r\Omega_{\rm K}-\alpha)[Q_{\rm s}^{+}(2\Omega_{\rm K}\tau, 2\hat{\theta}, 2\hat{\phi}) - \sin(2\Omega_{\rm K}\tau - 2\hat{\phi})]. \tag{64c}$$

Then the solutions to (41) and (43) are

$$S_{01}^{(1)}(\tau) = \frac{3}{16} m_0 r\left(\frac{s_0}{m_0 r}\right)^2 \frac{L_0}{N^3}\frac{(r^2\Omega_{\rm K}^2)(r\Omega_{\rm K}-\alpha)}{(1+\alpha r\Omega_{\rm K})}\{Q_{\rm c}^{+}(2\Omega_{\rm K}\tau, 2\hat{\theta}, 2\hat{\phi}) - Q_{\rm c}^{+}(0, 2\hat{\theta}, 2\hat{\phi}) - 2[\cos(2\Omega_{\rm K}\tau - 2\hat{\phi}) - \cos(2\hat{\phi})]\}, \tag{65a}$$

$$S_{02}^{(1)}(\tau) = \frac{3}{16} m_0 r^2\left(\frac{s_0}{m_0 r}\right)^2 \frac{L_0 A}{N^3}\frac{(r^2\Omega_{\rm K}^2)(r\Omega_{\rm K}-\alpha)}{(1+\alpha r\Omega_{\rm K})}\{(2\Omega_{\rm K}\tau)Q_{\rm c}^{-}(\Omega_{\rm K}\tau, 2\hat{\theta}, \hat{\phi}) - [Q_{\rm s}^{-}(\Omega_{\rm K}\tau, 2\hat{\theta}, \hat{\phi}) - Q_{\rm s}^{-}(0, 2\hat{\theta}, \hat{\phi})]\}, \tag{65b}$$

$$S_{03}^{(1)}(\tau) = -\frac{3}{8} m_0 r^2\left(\frac{s_0}{m_0 r}\right)^2 \frac{A^2}{N^2}(r\Omega_{\rm K})(r\Omega_{\rm K}-\alpha)\{Q_{\rm s}^{+}(2\Omega_{\rm K}\tau, 2\hat{\theta}, 2\hat{\phi}) - Q_{\rm s}^{+}(0, 2\hat{\theta}, 2\hat{\phi}) - 2[\sin(2\Omega_{\rm K}\tau - 2\hat{\phi}) + \sin(2\hat{\phi})]\}, \tag{65c}$$

$$S_{12}^{(1)}(\tau) = -\frac{3}{16} m_0 r^2\left(\frac{s_0}{m_0 r}\right)^2 \frac{L_0}{N^2 A}\frac{(r\Omega_{\rm K})(r\Omega_{\rm K}-\alpha)}{(1+\alpha r\Omega_{\rm K})}\{(2\Omega_{\rm K}\tau)Q_{\rm s}^{-}(\Omega_{\rm K}\tau, 2\hat{\theta}, \hat{\phi}) - [Q_{\rm c}^{-}(\Omega_{\rm K}\tau, 2\hat{\theta}, \hat{\phi}) - Q_{\rm c}^{-}(0, 2\hat{\theta}, \hat{\phi})]\}, \tag{65d}$$

$$S_{23}^{(1)}(\tau) = \frac{3}{16} m_0 r^3\left(\frac{s_0}{m_0 r}\right)^2 \frac{L_0 A}{N^3}(r\Omega_{\rm K})(r\Omega_{\rm K}-\alpha)\{(2\Omega_{\rm K}\tau)Q_{\rm c}^{-}(\Omega_{\rm K}\tau, 2\hat{\theta}, \hat{\phi}) - [Q_{\rm s}^{-}(\Omega_{\rm K}\tau, 2\hat{\theta}, \hat{\phi}) - Q_{\rm s}^{-}(0, 2\hat{\theta}, \hat{\phi})]\}, \tag{65e}$$

$$S_{31}^{(1)}(\tau) = -\frac{3}{16} m_0 r^2\left(\frac{s_0}{m_0 r}\right)^2 \frac{L_0}{N^3}(r\Omega_{\rm K})(r\Omega_{\rm K}-\alpha)\{Q_{\rm c}^{+}(2\Omega_{\rm K}\tau, 2\hat{\theta}, 2\hat{\phi}) - Q_{\rm c}^{+}(0, 2\hat{\theta}, 2\hat{\phi}) - 2[\cos(2\Omega_{\rm K}\tau - 2\hat{\phi}) - \cos(2\hat{\phi})]\}. \tag{65f}$$

When combined with (58), it follows that the first-order shift in the squared spin magnitude is

$$\bar{s}_1^2(\tau) = \frac{1}{N^2}\left(\frac{s_0}{m_0 r}\right)\tilde{s}_1^2(\tau), \tag{66}$$

where

$$\begin{aligned}\tilde{s}_1^2(\tau) = \frac{3}{16}\frac{L_0(r\Omega_{\rm K})(r\Omega_{\rm K}-\alpha)}{(1+\alpha r\Omega_{\rm K})}&\{(2\Omega_{\rm K}\tau)[Q_{\rm s}^{+}(2\Omega_{\rm K}\tau, 3\hat{\theta}, 2\hat{\phi}) - Q_{\rm s}^{+}(2\Omega_{\rm K}\tau, \hat{\theta}, 2\hat{\phi})] \\ &+ 3[Q_{\rm c}^{+}(2\Omega_{\rm K}\tau, 3\hat{\theta}, 2\hat{\phi}) - Q_{\rm c}^{+}(2\Omega_{\rm K}\tau, \hat{\theta}, 2\hat{\phi})] - Q_{\rm c}^{+}(\Omega_{\rm K}\tau, 3\hat{\theta}, 2\hat{\phi}) + Q_{\rm c}^{+}(\Omega_{\rm K}\tau, \hat{\theta}, 2\hat{\phi}) - Q_{\rm c}^{+}(\Omega_{\rm K}\tau, 3\hat{\theta}, 0) \\ &+ Q_{\rm c}^{+}(\Omega_{\rm K}\tau, \hat{\theta}, 0) - 2[Q_{\rm c}^{+}(0, 3\hat{\theta}, 2\hat{\phi}) - Q_{\rm c}^{+}(0, \hat{\theta}, 2\hat{\phi})] + 2[\cos(3\hat{\theta}) - \cos\hat{\theta}]\}.\end{aligned} \tag{67}$$

The time-averaged expression for (66) over a cycle defined by the Keplerian frequency is

$$\langle\bar{s}_1^2\rangle = \frac{1}{N^2}\left(\frac{s_0}{m_0 r}\right)\langle\tilde{s}_1^2\rangle, \tag{68}$$

where

$$\begin{aligned}\langle\tilde{s}_1^2\rangle &\equiv \frac{\Omega_{\rm K}}{2\pi}\int_0^{2\pi/\Omega_{\rm K}}\tilde{s}_1^2(\tau)d\tau \\ &= \frac{3}{2}\frac{L_0(r\Omega_{\rm K})(r\Omega_{\rm K}-\alpha)}{(1+\alpha r\Omega_{\rm K})}\sin^2\hat{\theta}\cos\hat{\theta}[3\cos(2\hat{\theta}) - 1].\end{aligned} \tag{69}$$

It is important to note that both (67) and (69) are well behaved for the full range of $\hat{\theta}$ and $\hat{\phi}$. However, there exists the possibility for singularities to appear in the limit as $(1+\alpha r\Omega_{\rm K}) \to 0$. This occurs when

$$r_{\rm c} \to \left(\frac{|a|}{M}\right)^{2/3} M, \qquad a < 0. \tag{70}$$

For the allowed radii permitted in the Kerr metric for photon orbits [30], it is clear that $r > r_{\rm c}$ for $a < 0$, so the relevant expressions considered here can never become singular.

It is more straightforward to solve for the remaining contributions to the perturbed Møller radius, $\bar{m}_2^2$ and $\bar{s}_2^2$, which are fourth-order perturbations in ε according to (17) and (18). The first nonzero "radiative correction" to the squared mass magnitude (17) is

$$\bar{m}^2_2(\tau) = \frac{9}{8}\frac{A^2}{N^4}\left(\frac{s_0}{m_0 r}\right)^2 (r^2\Omega_{\rm K}^2)(r\Omega_{\rm K} - \alpha)^2 \times \{Q_{\rm c}^+(2\Omega_{\rm K}\tau, 2\hat{\theta}, 2\hat{\phi}) - Q_{\rm c}^+(0, 2\hat{\theta}, 2\hat{\phi}) - 2[\cos(2\Omega_{\rm K}\tau - 2\hat{\phi}) - \cos(2\hat{\phi})]\}, \quad (71)$$

according to (19), where its time-averaged expression following the definition given in (69) is

$$\langle \bar{m}^2_2 \rangle = \frac{9}{2}\frac{A^2}{N^4}\left(\frac{s_0}{m_0 r}\right)^2 (r^2\Omega_{\rm K}^2)(r\Omega_{\rm K} - \alpha)^2 \sin^2\hat{\theta}(2\cos^2\hat{\theta} - 1). \quad (72)$$

It is clear that the expressions (71) and (72) for $\bar{m}^2_2$ have no coordinate singularities due to $\hat{\theta}$ and $\hat{\phi}$, nor are there any physical singularities for reasonable choices for r.

As for $\bar{s}^2_2$, it follows from evaluating (20) for $j = 2$ that

$$\bar{s}^2_2(\tau) = -\frac{3A^2}{8N^4}\left(\frac{s_0}{m_0 r}\right)(r^2\Omega_{\rm K}^2)(r\Omega_{\rm K} - \alpha)(1 + \alpha r\Omega_{\rm K})[Q_{\rm c}^+(4\Omega_{\rm K}\tau, 3\hat{\theta}, 2\hat{\phi}) - Q_{\rm c}^+(4\Omega_{\rm K}\tau, \hat{\theta}, 2\hat{\phi}) - Q_{\rm c}^+(3\Omega_{\rm K}\tau, 3\hat{\theta}, 2\hat{\phi}) + Q_{\rm c}^+(3\Omega_{\rm K}\tau, \hat{\theta}, 2\hat{\phi}) + 3Q_{\rm c}^+(3\Omega_{\rm K}\tau, 3\hat{\theta}, 0) + 5Q_{\rm c}^+(3\Omega_{\rm K}\tau, \hat{\theta}, 0) + Q_{\rm c}^+(\Omega_{\rm K}\tau, 3\hat{\theta}, -2\hat{\phi}) - 3Q_{\rm c}^+(\Omega_{\rm K}\tau, 3\hat{\theta}, 0) - Q_{\rm c}^+(\Omega_{\rm K}\tau, \hat{\theta}, -2\hat{\phi}) - 5Q_{\rm c}^+(\Omega_{\rm K}\tau, \hat{\theta}, 0) - Q_{\rm c}^+(0, 3\hat{\theta}, 2\hat{\phi}) + Q_{\rm c}^+(0, \hat{\theta}, 2\hat{\phi})], \quad (73)$$

whose time-averaged expression is

$$\langle \bar{s}^2_2 \rangle = -\frac{3A^2}{N^4}\left(\frac{s_0}{m_0 r}\right)(r^2\Omega_{\rm K}^2)(r\Omega_{\rm K} - \alpha)(1 + \alpha r\Omega_{\rm K}) \times \sin^2\hat{\theta}\cos\hat{\theta}(2\cos^2\hat{\phi} - 1). \quad (74)$$

Again, (73) and (74) for $\bar{s}^2_2$ indicate well-behaved functions for all choices of $\hat{\theta}$ and $\hat{\phi}$, with no possibility of encountering singularities of any kind. It is interesting to note, however, that $\bar{s}^2_2$ is *linear* in $s_0/(m_0 r)$, the same order as found in (66) for $\bar{s}^2_1$, which is somewhat unexpected. Furthermore, for $N \to 0$, it appears at first glance that $\bar{s}^2_2$ will dominate over $\bar{s}^2_1$. Though it is difficult to identify the source for these unusual features, this may be indicative of another classical analogy to nonrenormalizability in quantum field theory, where higher-order perturbation terms in the generalized CMP approximation may possibly contribute to *all orders* of the expansion for certain quantities. This is a matter which may require further study in the future.

V. NUMERICAL ANALYSIS

At this point, it is useful to consider some numerical analysis of the main expressions for this paper, which are found in Appendix B of this paper. The purpose behind this procedure is to get a visual sense for how increasing the order of the perturbation expansion in the generalized CMP approximation influences the predicted physical behavior of the spinning particle in the Kerr background. Since a purely numerical approach to the MPD equations does not allow for the clear identification of dominant contributions to the particle's orbital motion, this treatment provides an opportunity to glean some insight as to where a correspondence between the two approaches may occur.

For all plots presented, $r = 6M$ and $\hat{\theta} = \hat{\phi} = \pi/4$. Particular attention is given to understanding the general stability of the spinning particle's motion while in circular orbit around a Kerr black hole, especially given the "radiative corrections" of the squared mass and spin magnitudes denoted by (19) and (20), respectively.

For the purposes of this paper, $\mu \equiv s_0/(m_0 r) = 10^{-2}$ and $\mu = 10^{-1}$ are considered throughout, where $m_0 = 10^{-2}M$. It so happens that, for the given choices of r and m_0, it follows that

$$s_0 = \left(10^2\frac{r\mu}{M}\right)m_0^2. \quad (75)$$

This implies that a realistic spin of $s_0 \lesssim m_0^2$ for solar mass black holes and neutron stars [13,31] orbiting supermassive black holes requires that

$$\mu \lesssim 10^{-2}\frac{M}{r}. \quad (76)$$

This upper bound given by (76) indicates that the choices of $\mu = 10^{-2}$ and $\mu = 10^{-1}$ correspond to unrealistically large values [13,14] for s_0, and consistent with values chosen in previous work [11,12] suggesting chaotic behavior for the MPD equations. Therefore, any chaotic phenomena reported in this paper occurs under conditions not expected to be realized in a realistic astrophysical setting.

To begin, consider the magnitude for the particle's coordinate speed

$$v(\varepsilon) = \sqrt{g_{ij}V^i(\varepsilon)V^j(\varepsilon)}, \quad (77)$$

where

$$V^i(\varepsilon) \equiv \frac{u^i(\varepsilon)}{u^0(\varepsilon)}, \tag{78}$$

and the $u^\mu(\varepsilon)$ are given by (25). Since it must be true that $0 \leq v < 1$, it follows that any violation of this range of validity reflects a breakdown of the formalism's applicability. An exploration of (77) is presented in Fig. 1, to first and second order in ε, for the special cases of corotating ($a = M$) and counterrotating ($a = -M$) extreme Kerr black holes. It is important to note that while $r = 6M$ corresponds to stable orbital motion for a spinless particle when $a = M$, this choice for r only leads to marginally bounded orbits when $a = -M$ [30].

For Figs. 1(a) and 1(b), the choice of $s_0/(m_0 r) = 10^{-2}$ shows that the spin-curvature force acting on the particle's motion is almost exclusively due to the expression to first order in ε. In particular, the overall motion is stable throughout the range considered, with a variation on the order of 10^{-3} for Fig. 1(a) and 10^{-2} for Fig. 1(b), where the $O(\varepsilon^2)$ expression only yields a 2×10^{-3} increase at the end of the plot compared to the first-order contribution alone. However, when $s_0/(m_0 r) = 10^{-1}$, the situation changes dramatically for both cases of a, as illustrated by Figs. 1(c) and 1(d). This is because the second-order expression in ε introduces a rapid increase in the coordinate speed that approaches the $v = 1$ upper bound. It is par-

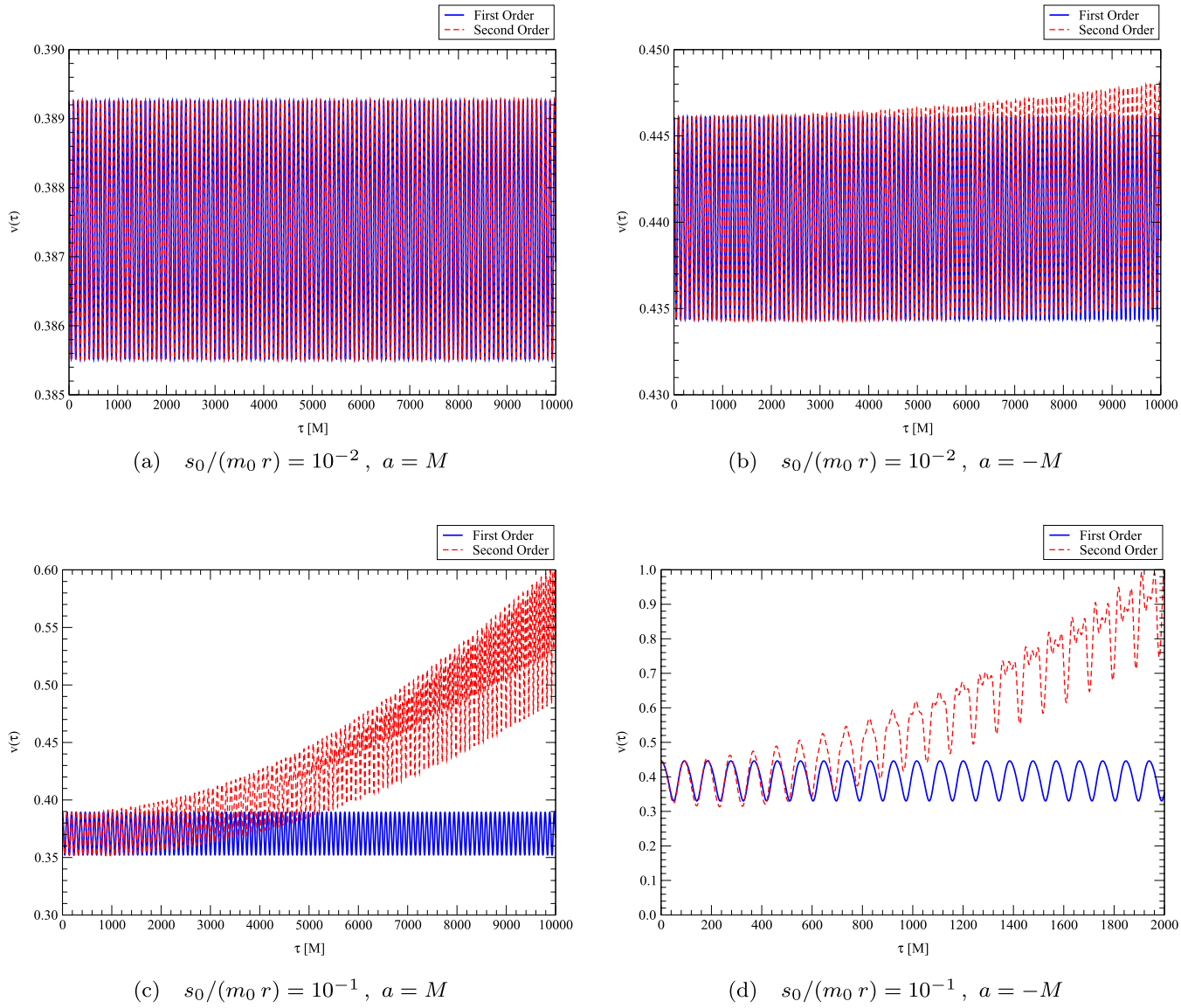

FIG. 1 (color online). Coordinate speed $v(\tau)$ of the spinning particle while in circular orbit around a Kerr black hole, for $r = 6M$ and $\hat{\theta} = \hat{\phi} = \pi/4$. It is clear from (a) that $v(\tau)$ to second-order contribution in ε has no significant impact on altering the particle's orbital speed for $s_0/(m_0 r) = 10^{-2}$, though (b) indicates a slight increase over time. In contrast, (c) and (d) show that an instability occurs as $s_0/(m_0 r) = 10^{-1}$ when considering the second-order contribution of ε in $v(\tau)$.

ticularly evident to see this in Fig. 1(d), which formally exceeds $v(\tau) = 1$ for $\tau > 2000M$. Such an outcome for Figs. 1(c) and 1(d) is consistent with prior numerical analysis on orbital stability [11,13] when considering large initial spin magnitudes s_0.

For immediate comparison, it is useful to now consider the Møller radius $\rho(\tau) = (s/m)(\tau)$ given by (27) for the same set of initial conditions. The purpose of this analysis is to determine whether a correlation exists between the kinematic effects in $v(\tau)$ with the anticipated dynamical contributions due to the spin-curvature interaction in $\rho(\tau)$. Figure 2 is a plot of the Møller radius in units of s_0/m_0, up to $O(\varepsilon^3)$, for $a = M$ and $a = -M$. Comparison with Fig. 1 suggests that such a correlation exists between the two plots. The expression to third order in ε, which includes the mass shift contribution $\bar{m}_2^2$ as well as the second-order spin shift term $\bar{s}_2^2$, has the effect of shifting the range of oscillation downwards within the plots as compared to the second-order expression alone, which oscillates with growing amplitude about $\rho = 1$.

According to Fig. 2(a) for $s_0/(m_0 r) = 10^{-2}$ and $a = M$, the amplitude for Møller radius grows very slowly when compared to Fig. 2(b) for $s_0/(m_0 r) = 10^{-2}$ and $a = -M$. Both the growth of the amplitude and the downward shift of the plots become more pronounced when examining Figs. 2(c) and 2(d) for $a = M$ and $a = -M$, respectively, when $s_0/(m_0 r) = 10^{-1}$. In particular, the amplitude becomes many times larger than $\rho_0 = s_0/m_0 = 1$ for both the corotating and counterrotating black hole cases, which suggests that a certain minimum value for $\rho(\tau)$ must occur before instability of the orbital motion appears. Though the Møller radius is not apparently a geometric quantity that must necessarily be positive valued, it is interesting to note that the rapid increase in $v(\tau)$ roughly coincides with the condition that $\rho(\tau) < 0$ for each of the plots in Fig. 2. This may be a useful criterion for helping to determine the occurrence of instabilities in the spinning particle's orbital motion.

A further consideration involving the Møller radius is to examine its time-averaged value $\langle\rho\rangle = \langle s/m\rangle$ as a function of the initial spin orientation angles $\hat{\theta}$ and $\hat{\phi}$. This leads to three-dimensional plots described by Figs. 3 and 4 for $a = M$ and $a = -M$, respectively, which display expressions to both second and third order in ε for $\langle\rho\rangle$, and where $s_0/(m_0 r) = 10^{-1}$. It is evident that all the plots reflect an even function symmetry with respect to $\hat{\phi} = \pi$. According to Figs. 3(a) and 4(a), the $O(\varepsilon^2)$ expressions lead to a nontrivial peak and valley structure in $\langle\rho\rangle$, while Figs. 3(b) and 4(b) for third order in ε effectively removes some of the structure for the region defined by $0 \le \hat{\theta} < \pi$, leaving two peaks to dominate. While the shapes of the three-dimensional plots are effectively unchanged when comparing between Figs. 3 and 4, going from $a = M$ to $a = -M$ leads to a tenfold increase in magnitude, suggesting as expected that the counterrotating black hole for $r = 6M$ leads to a greater likelihood for encountering instabilities within the spinning particle's orbit.

It is useful to briefly examine the linear momentum components $P^\mu(\tau)$, given (33) and (44). Figures 5–7 display the radial, polar, and azimuthal components of the linear momentum, while Fig. 8 displays the ratio $P^3(\tau)/P^0(\tau)$, such as that described to first order in ε according to (60). For the radial component corresponding to $s_0/(m_0 r) = 10^{-2}$, Fig. 5(a) for $a = M$ shows that the expression to second order in ε introduces a slight contraction in the amplitude of $P^1(\tau)$ before expanding outwards. This behavior is also present in Fig. 5(b) for $a = -M$, though the outward growth is more pronounced, the beginning of which roughly corresponds with the increase in $v(\tau)$ in Fig. 1(b) starting at $\tau = 3000M$. Not surprisingly, the $O(\varepsilon^2)$ expression becomes dominant in Figs. 5(c) and 5(d) when $s_0/(m_0 r) = 10^{-1}$, which also corresponds with the respective increases in $v(\tau)$, as found in Figs. 1(c) and 1(d).

The polar component corresponding to $s_0/(m_0 r) = 10^{-2}$ is described by Fig. 6(a) for $a = M$ and Fig. 6(b) for $a = -M$, which indicate a slightly net positive magnitude in $P^2(\tau)$ due to the expression to second order in ε. This outcome is somewhat surprising, since this suggests that the spinning particle will permanently leave the equatorial plane under these conditions. However, this may be more reflective of the choice for r, which hovers around the minimum value allowable for stable circular orbits. Again, this outcome is more pronounced for the case of $s_0/(m_0 r) = 10^{-1}$, as shown in Figs. 6(c) and 6(d).

For the azimuthal component corresponding to $s_0/(m_0 r) = 10^{-2}$, Fig. 7 behaves similarly to that of Fig. 5, particularly where it concerns Figs. 7(a) and 7(b) for $a = M$ and $a = -M$, respectively. That is, the $O(\varepsilon^2)$ expression indicates a slight contraction in the amplitude of $P^3(\tau)$ prior to an outward expansion. Consistent with previous plots, Figs. 7(c) and 7(d) show a dominant growth of the amplitude of $P^3(\tau)$ for the expression to second order in ε and $s_0/(m_0 r) = 10^{-1}$.

Concerning the ratio $P^3(\tau)/P^0(\tau)$, this is presented in Fig. 8 for the case of $s_0/(m_0 r) = 10^{-2}$, where Fig. 8(a) refers to $a = M$ and Fig. 8(b) corresponds to $a = -M$. As expected, the first-order contribution in ε leads to a constant ratio in τ, consistent with (60). When the second-order contribution in ε is added, the ratio exhibits a slight contraction followed by an outward expansion, consistent with Figs. 7(a) and 7(b) for $P^3(\tau)$. Nonetheless, it appears that the basic ratio remains constant for changing τ.

Finally, to explore the numerical properties of the spin tensor due to the generalized CMP approximation, consider the example of $S^{02}(\tau)$, as presented in Fig. 9, which shows expressions up to third order in ε. It seems evident that the expression to second order in ε is dominant, as then it is clear that the $O(\varepsilon^3)$ expression has no discernible impact on the amplitude. According to Fig. 9(a) for

$s_0/(m_0 r) = 10^{-2}$ and $a = M$, the amplitude remains constant around $S^{02}(\tau) = 0$, while Fig. 9(b) for $a = -M$ shows a gradual growth in the amplitude. Consistent with previous plots, this effect becomes more pronounced in Figs. 9(c) and 9(d) for $s_0/(m_0 r) = 10^{-1}$.

VI. CONCLUSION

This paper outlines the generalization of an analytic perturbation approach to the Mathisson-Papapetrou-Dixon equations for a spinning point particle, first introduced by Chicone, Mashhoon, and Punsly, with an application to circular motion around a Kerr black hole. The formalism shows the existence of ''radiative corrections'' to the particle's squared mass and spin magnitudes due to spin-curvature interactions, represented in power series expansion form. In performing the analysis, it is possible to semianalytically identify the emergence of instabilities during the particle's orbital motion, which serves as a basis for a more precise treatment in the future.

One of the underlying goals of the formalism presented in this paper is to determine the perturbed orbit of the spinning particle according to the generalized CMP approximation, following the approach taken earlier [21]. However, to do this properly requires a modification of the equations of motion to incorporate dissipative effects due to gravitational radiation, which have not yet been taken into account. Such a modification would most certainly require evaluation of the Teukolsky equations for determining the radiation effects corresponding to an adiabatic inspiral for the spinning particle's orbit. This is a nontrivial exercise with both conceptual and technical challenges to still overcome. Once this is better understood, a determination of the perturbed orbit due to spin-curvature interactions will be considered in a future publication. For now, a second paper on the generalized CMP approximation in the Vaidya background is forthcoming [32] as a companion piece to accompany and compare with this paper.

ACKNOWLEDGMENTS

The author is thankful to Professor Nader Mobed of the University of Regina for financial and moral support towards the completion of this project.

APPENDIX A: FERMI-FRAME RIEMANN TENSOR COMPONENTS

Given that the nonzero Riemann curvature tensor components in standard Boyer-Lindquist coordinates are

$$R_{0101} = -\frac{Mr}{\Sigma^3\Delta}(\Sigma - 4a^2\cos^2\theta)(2\Delta + a^2\sin^2\theta), \quad \text{(A1)}$$

$$R_{0102} = \frac{3Ma^2}{\Sigma^3}(4r^2 - \Sigma)\sin\theta\cos\theta, \quad \text{(A2)}$$

$$R_{0113} = -\frac{Mar}{\Sigma^3\Delta}(4r^2 - 3\Sigma)(r^2 + a^2 + 2\Delta)\sin^2\theta, \quad \text{(A3)}$$

$$R_{0123} = \frac{Ma}{\Sigma^3}(4r^2 - \Sigma)(2\Sigma + 3a^2\sin^2\theta)\sin\theta\cos\theta, \quad \text{(A4)}$$

$$R_{0202} = \frac{Mr}{\Sigma^3}(4r^2 - 3\Sigma)(\Delta + 2a^2\sin^2\theta), \quad \text{(A5)}$$

$$R_{0213} = \frac{Ma}{\Sigma^3}(4r^2 - \Sigma)(\Sigma + 3a^2\sin^2\theta)\sin\theta\cos\theta, \quad \text{(A6)}$$

$$R_{0223} = \frac{Mar}{\Sigma^3}(4r^2 - 3\Sigma)[2(r^2 + a^2) + \Delta]\sin^2\theta, \quad \text{(A7)}$$

$$R_{0303} = \frac{Mr\Delta}{\Sigma^3}(4r^2 - 3\Sigma)\sin^2\theta, \quad \text{(A8)}$$

$$R_{0312} = -\frac{Ma}{\Sigma^2}(4r^2 - \Sigma)\sin\theta\cos\theta, \quad \text{(A9)}$$

$$R_{1212} = -\frac{Mr}{\Sigma\Delta}(4r^2 - 3\Sigma), \quad \text{(A10)}$$

$$R_{1313} = -\frac{Mr}{\Sigma^3\Delta}(4r^2 - 3\Sigma)[(r^2 + a^2)^2 + 2a^2\Delta\sin^2\theta]\sin^2\theta, \quad \text{(A11)}$$

$$R_{1323} = \frac{3Ma^2}{\Sigma^3}(4r^2 - \Sigma)(r^2 + a^2)\sin^3\theta\cos\theta, \quad \text{(A12)}$$

$$R_{2323} = \frac{Mr}{\Sigma^3}(4r^2 - 3\Sigma)[2(r^2 + a^2)^2 + a^2\Delta\sin^2\theta]\sin^2\theta, \quad \text{(A13)}$$

where

$$\Sigma = r^2 + a^2\cos^2\theta, \quad \text{(A14)}$$

$$\Delta = r^2 + a^2 - 2Mr, \quad \text{(A15)}$$

the nonzero components of the Riemann curvature tensor ${}^F R_{\hat{\mu}\hat{\nu}\hat{\alpha}\hat{\beta}}$ in the Fermi frame are listed as follows:

$$\begin{aligned} {}^F R_{\hat{0}\hat{1}\hat{0}\hat{1}} = {} & \frac{\Delta}{N^2 r^2}\left[(1 + a\Omega_K)^2 R_{0101} - \frac{2\Omega_K}{\sin\theta}(1 + a\Omega_K)R_{0113} + \frac{\Omega_K^2}{\sin^2\theta}R_{1313}\right]\cos^2(\Omega_K\tau) \\ & + \frac{1}{N^2\Delta\sin^2\theta}[E + \Omega_K(aE - L)]^2 R_{0303}\sin^2(\Omega_K\tau), \end{aligned} \quad \text{(A16)}$$

$$ {}^{F}R_{\hat{0}\hat{1}\hat{0}\hat{2}} = \frac{\sqrt{\Delta}}{N^2 r^2}\left[(1+a\Omega_{\mathrm{K}})^2 R_{0102} - \frac{\Omega_{\mathrm{K}}}{\sin\theta}(1+a\Omega_{\mathrm{K}})(R_{0213}+R_{0123}) + \frac{\Omega_{\mathrm{K}}^2}{\sin^2\theta}R_{1323}\right]\cos(\Omega_{\mathrm{K}}\tau), \tag{A17} $$

$$ {}^{F}R_{\hat{0}\hat{1}\hat{0}\hat{3}} = \frac{1}{N^2\sin\theta}\left\{\frac{\Delta}{r^2}\left[(1+a\Omega_{\mathrm{K}})[(1+a\Omega_{\mathrm{K}})\sin\theta R_{0101} - 2\Omega_{\mathrm{K}}R_{0113}] + \frac{\Omega_{\mathrm{K}}^2}{\sin\theta}R_{1313}\right] - \frac{1}{\Delta\sin\theta}[E+\Omega_{\mathrm{K}}(aE-L)]^2 R_{0303}\right\} \times \sin(\Omega_{\mathrm{K}}\tau)\cos(\Omega_{\mathrm{K}}\tau), \tag{A18} $$

$$ {}^{F}R_{\hat{0}\hat{1}\hat{1}\hat{2}} = \frac{1}{Nr^2}\left\{(1+a\Omega_{\mathrm{K}})\left(\frac{E}{\sin\theta}R_{0123} - LR_{0102}\right) - \frac{\Omega_{\mathrm{K}}}{\sin\theta}\left(\frac{E}{\sin\theta}R_{1323} - LR_{0213}\right) - \frac{1}{\sin\theta}[E+\Omega_{\mathrm{K}}(aE-L)]R_{0312}\right\} \times \sin(\Omega_{\mathrm{K}}\tau)\cos(\Omega_{\mathrm{K}}\tau), \tag{A19} $$

$$ {}^{F}R_{\hat{0}\hat{1}\hat{1}\hat{3}} = \frac{\sqrt{\Delta}}{Nr^2}\left\{\frac{1}{\sin\theta}[E+\Omega_{\mathrm{K}}(aE+L)]R_{0113} - \left[\frac{\Omega_{\mathrm{K}}E}{\sin^2\theta}R_{1313} + (1+a\Omega_{\mathrm{K}})LR_{0101}\right]\right\}\cos(\Omega_{\mathrm{K}}\tau), \tag{A20} $$

$$ {}^{F}R_{\hat{0}\hat{1}\hat{2}\hat{3}} = \frac{1}{Nr^2}\left\{\left[(1+a\Omega_{\mathrm{K}})\left(\frac{E}{\sin\theta}R_{0123} - LR_{0102}\right) - \frac{\Omega_{\mathrm{K}}}{\sin\theta}\left(\frac{E}{\sin\theta}R_{1323} - LR_{0213}\right)\right]\cos^2(\Omega_{\mathrm{K}}\tau) + \frac{1}{\sin\theta}[E+\Omega_{\mathrm{K}}(aE-L)]R_{0312}\sin^2(\Omega_{\mathrm{K}}\tau)\right\}, \tag{A21} $$

$$ {}^{F}R_{\hat{0}\hat{2}\hat{0}\hat{2}} = \frac{1}{N^2 r^2}\left[(1+a\Omega_{\mathrm{K}})^2 R_{0202} - \frac{2\Omega_{\mathrm{K}}}{\sin\theta}(1+a\Omega_{\mathrm{K}})R_{0223} + \frac{\Omega_{\mathrm{K}}^2}{\sin^2\theta}R_{2323}\right], \tag{A22} $$

$$ {}^{F}R_{\hat{0}\hat{2}\hat{0}\hat{3}} = \frac{\sqrt{\Delta}}{N^2 r^2}\left\{(1+a\Omega_{\mathrm{K}})\left[(1+a\Omega_{\mathrm{K}})R_{0102} - \frac{\Omega_{\mathrm{K}}}{\sin\theta}(R_{0123}+R_{0213})\right] + \frac{\Omega_{\mathrm{K}}^2}{\sin^2\theta}R_{1323}\right\}\sin(\Omega_{\mathrm{K}}\tau), \tag{A23} $$

$$ {}^{F}R_{\hat{0}\hat{2}\hat{1}\hat{2}} = \frac{1}{N\sqrt{\Delta}r^2}\left\{\frac{1}{\sin\theta}[E+\Omega_{\mathrm{K}}(aE+L)]R_{0223} - \left[\frac{\Omega_{\mathrm{K}}E}{\sin^2\theta}R_{2323} + (1+a\Omega_{\mathrm{K}})LR_{0202}\right]\right\}\sin(\Omega_{\mathrm{K}}\tau), \tag{A24} $$

$$ {}^{F}R_{\hat{0}\hat{2}\hat{1}\hat{3}} = \frac{1}{Nr^2}\left[(1+a\Omega_{\mathrm{K}})\left(\frac{E}{\sin\theta}R_{0213} - LR_{0102}\right) - \frac{\Omega_{\mathrm{K}}}{\sin\theta}\left(\frac{E}{\sin\theta}R_{1323} - LR_{0123}\right)\right], \tag{A25} $$

$$ {}^{F}R_{\hat{0}\hat{2}\hat{2}\hat{3}} = \frac{1}{N\sqrt{\Delta}r^2}\left\{\frac{1}{\sin\theta}[E+\Omega_{\mathrm{K}}(aE+L)]R_{0223} - \left[\frac{\Omega_{\mathrm{K}}E}{\sin^2\theta}R_{2323} + (1+a\Omega_{\mathrm{K}})LR_{0202}\right]\right\}\cos(\Omega_{\mathrm{K}}\tau), \tag{A26} $$

$$ {}^{F}R_{\hat{0}\hat{3}\hat{0}\hat{3}} = \frac{\Delta}{N^2 r^2}\left[(1+a\Omega_{\mathrm{K}})^2 R_{0101} - \frac{2\Omega_{\mathrm{K}}}{\sin\theta}(1+a\Omega_{\mathrm{K}})R_{0113} + \frac{\Omega_{\mathrm{K}}^2}{\sin^2\theta}R_{1313}\right]\sin^2(\Omega_{\mathrm{K}}\tau) + \frac{1}{N^2\Delta\sin^2\theta}[E+\Omega_{\mathrm{K}}(aE-L)]^2 R_{0303}\cos^2(\Omega_{\mathrm{K}}\tau), \tag{A27} $$

$$ {}^{F}R_{\hat{0}\hat{3}\hat{1}\hat{2}} = \frac{1}{Nr^2}\left\{\left[(1+a\Omega_{\mathrm{K}})\left(\frac{E}{\sin\theta}R_{0123} - LR_{0102}\right) - \frac{\Omega_{\mathrm{K}}}{\sin\theta}\left(\frac{E}{\sin\theta}R_{1323} - LR_{0213}\right)\right]\sin^2(\Omega_{\mathrm{K}}\tau) + \frac{1}{\sin\theta}[E+\Omega_{\mathrm{K}}(aE-L)]R_{0312}\cos^2(\Omega_{\mathrm{K}}\tau)\right\}, \tag{A28} $$

$$ {}^{F}R_{\hat{0}\hat{3}\hat{1}\hat{3}} = \frac{\sqrt{\Delta}}{Nr^2}\left\{\frac{1}{\sin\theta}[E+\Omega_{\mathrm{K}}(aE+L)]R_{0113} - \left[\frac{\Omega_{\mathrm{K}}E}{\sin^2\theta}R_{1313} + (1+a\Omega_{\mathrm{K}})LR_{0101}\right]\right\}\sin(\Omega_{\mathrm{K}}\tau), \tag{A29} $$

$$ {}^{F}R_{\hat{0}\hat{3}\hat{2}\hat{3}} = \frac{1}{Nr^2}\left\{(1+a\Omega_{\mathrm{K}})\left(\frac{E}{\sin\theta}R_{0123} - LR_{0102}\right) - \frac{\Omega_{\mathrm{K}}}{\sin\theta}\left(\frac{E}{\sin\theta}R_{1323} - LR_{0213}\right) - \frac{1}{\sin\theta}[E+\Omega_{\mathrm{K}}(aE-L)]R_{0312}\right\} \times \sin(\Omega_{\mathrm{K}}\tau)\cos(\Omega_{\mathrm{K}}\tau), \tag{A30} $$

$$ {}^{F}R_{\hat{1}\hat{2}\hat{1}\hat{2}} = \frac{1}{\Delta r^2}\left[\frac{E}{\sin\theta}\left(\frac{E}{\sin\theta}R_{2323} - 2LR_{0223}\right) + L^2R_{0202}\right]\sin^2(\Omega_K\tau) + \frac{\Delta}{r^4}R_{1212}\cos^2(\Omega_K\tau), \tag{A31} $$

$$ {}^{F}R_{\hat{1}\hat{2}\hat{1}\hat{3}} = \frac{1}{\sqrt{\Delta}r^2}\left[\frac{E}{\sin\theta}\left(\frac{E}{\sin\theta}R_{1323} - LR_{0123}\right) - L\left(\frac{E}{\sin\theta}R_{0213} - LR_{0102}\right)\right]\sin^2(\Omega_K\tau), \tag{A32} $$

$$ {}^{F}R_{\hat{1}\hat{2}\hat{2}\hat{3}} = \left\{\frac{1}{\Delta r^2}\left[\frac{E}{\sin\theta}\left(\frac{E}{\sin\theta}R_{2323} - 2LR_{0223}\right) + L^2R_{0202}\right] - \frac{\Delta}{r^4}R_{1212}\right\}\sin(\Omega_K\tau)\cos(\Omega_K\tau), \tag{A33} $$

$$ {}^{F}R_{\hat{1}\hat{3}\hat{1}\hat{3}} = \frac{1}{r^2}\left[\frac{E}{\sin\theta}\left(\frac{E}{\sin\theta}R_{1313} - 2LR_{0113}\right) + L^2R_{0101}\right], \tag{A34} $$

$$ {}^{F}R_{\hat{1}\hat{3}\hat{2}\hat{3}} = \frac{1}{\sqrt{\Delta}r^2}\left\{\frac{E}{\sin\theta}\left[\frac{E}{\sin\theta}R_{1323} - L(R_{0123} + R_{0213})\right] + L^2R_{0102}\right\}\cos(\Omega_K\tau), \tag{A35} $$

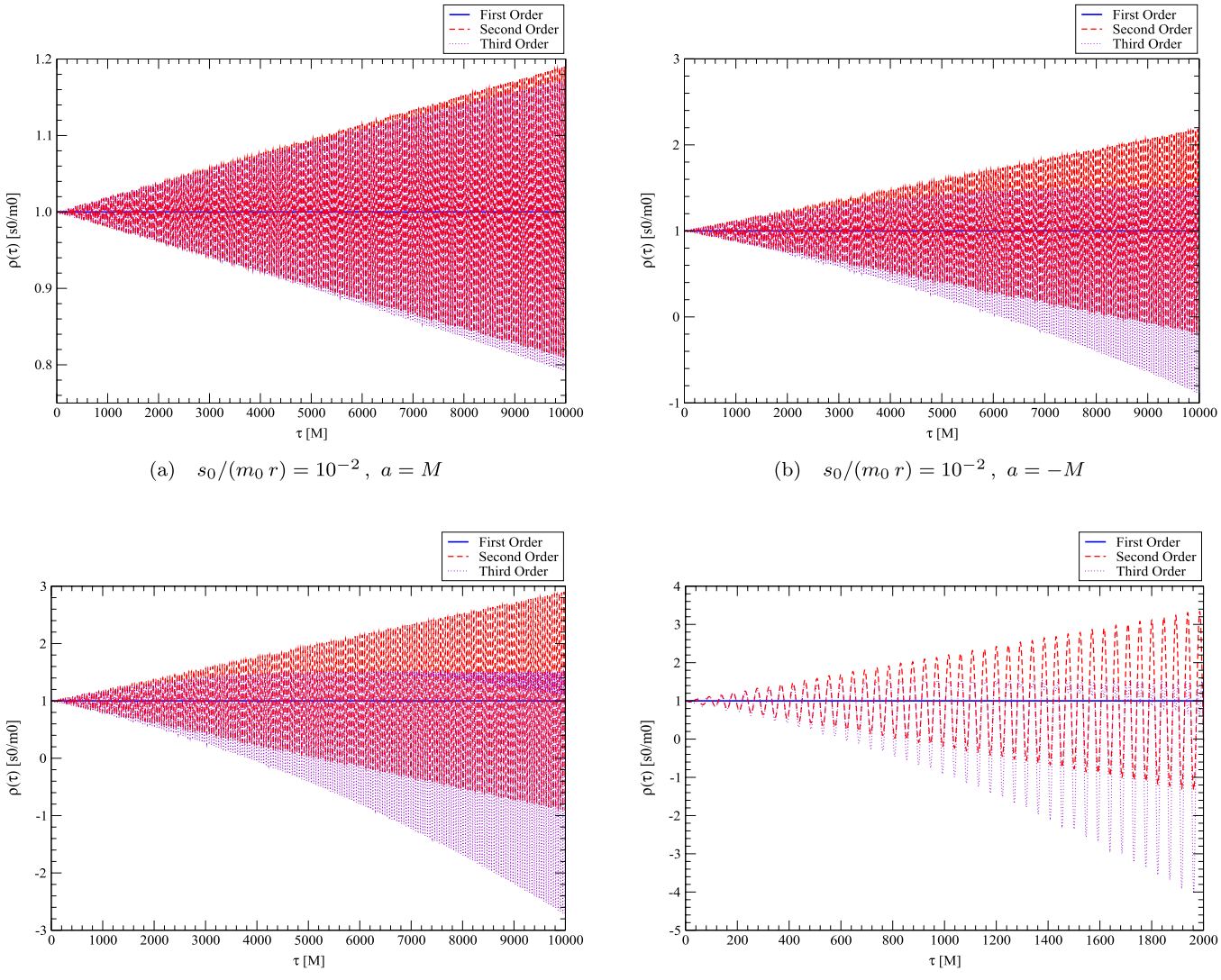

(a) $s_0/(m_0\,r) = 10^{-2}\,,\ a = M$ (b) $s_0/(m_0\,r) = 10^{-2}\,,\ a = -M$

(c) $s_0/(m_0\,r) = 10^{-1}\,,\ a = M$ (d) $s_0/(m_0\,r) = 10^{-1}\,,\ a = -M$

FIG. 2 (color online). Møller radius $\rho(\tau) = (s/m)(\tau)$ for $r = 6M$ and $\hat{\theta} = \hat{\phi} = \pi/4$, in units of s_0/m_0. (a) shows that while the higher-order contributions in ε lead to a slowly increasing amplitude in ρ, with a moderate increase found in (b). As $s_0/(m_0 r) = 10^{-1}$, the amplitude increase becomes more pronounced for (c) and (d), where the second- and third-order contributions in ε are noticeable.

$$^{F}R_{\hat{2}\hat{3}\hat{2}\hat{3}} = \frac{1}{\Delta r^2}\left[\frac{E}{\sin\theta}\left(\frac{E}{\sin\theta}R_{2323} - 2LR_{0223}\right) + L^2R_{0202}\right]\cos^2(\Omega_K\tau) + \frac{\Delta}{r^4}R_{1212}\sin^2(\Omega_K\tau). \tag{A36}$$

APPENDIX B: SELECTED PLOTS FOR THE GENERALIZED CMP APPROXIMATION OF THE MPD EQUATIONS

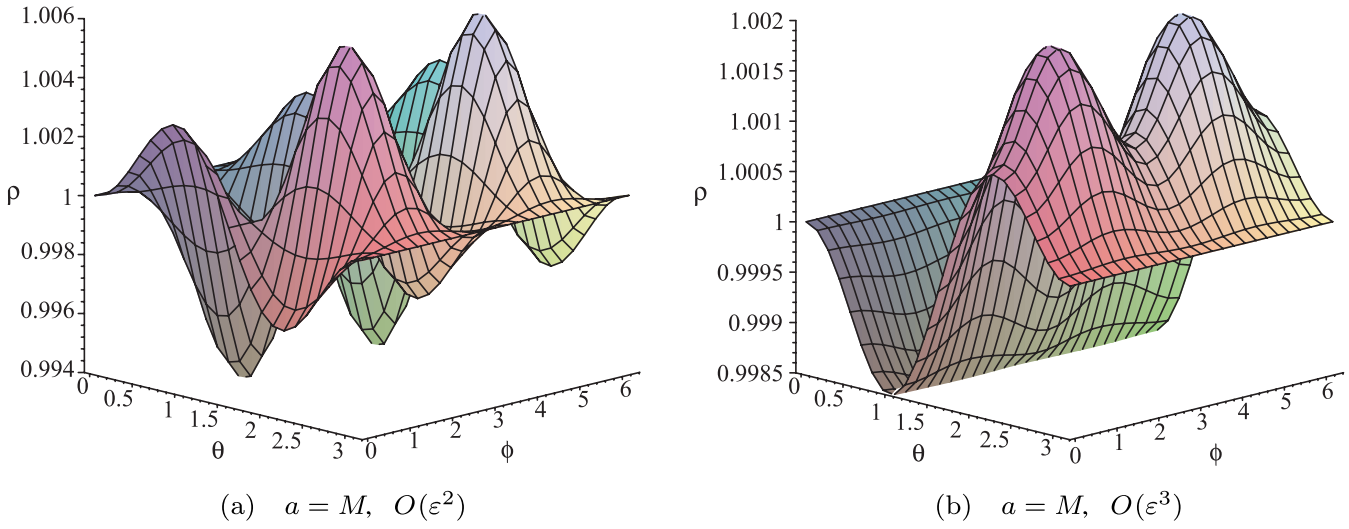

FIG. 3 (color online). Three-dimensional plot of the time-averaged Møller radius $\langle\rho\rangle = \langle s/m\rangle$ in units of s_0/m_0 as a function of $\hat{\theta}$ and $\hat{\phi}$ for $r = 6M$ and $a = M$. (a) shows a complicated peak and valley structure to $\langle\rho\rangle$ that simplifies somewhat in (b), with two peaks present.

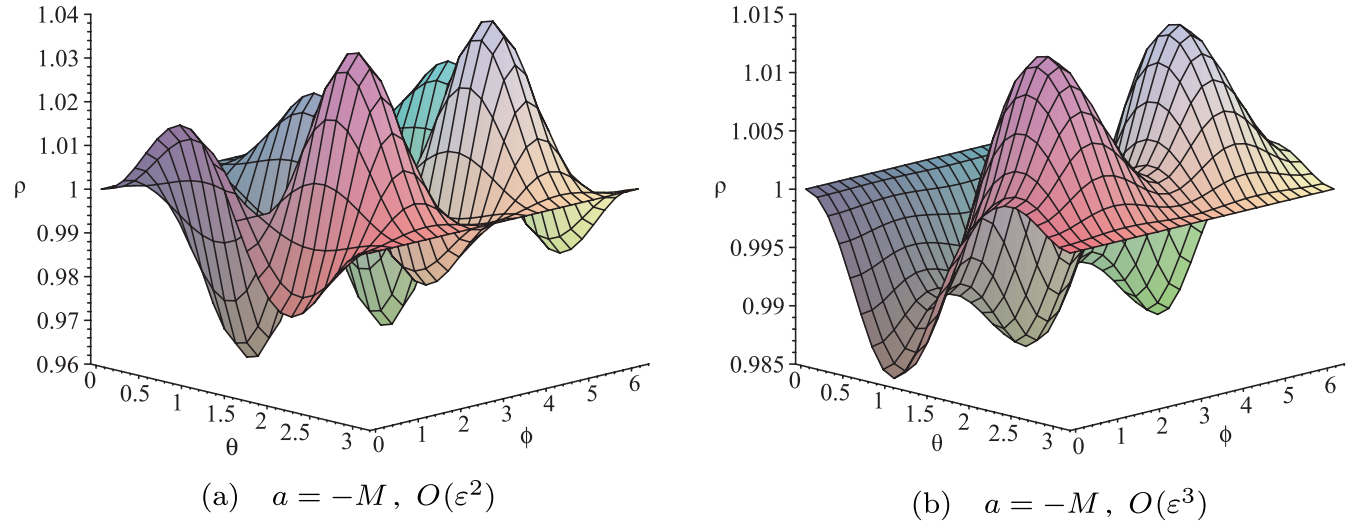

FIG. 4 (color online). Time-averaged Møller radius as a function of $\hat{\theta}$ and $\hat{\phi}$ for $r = 6M$ and $a = -M$. It is clear that while the peak structure is essentially unchanged when compared to Fig. 3, the magnitude increases tenfold when going from $a = M$ to $a = -M$.

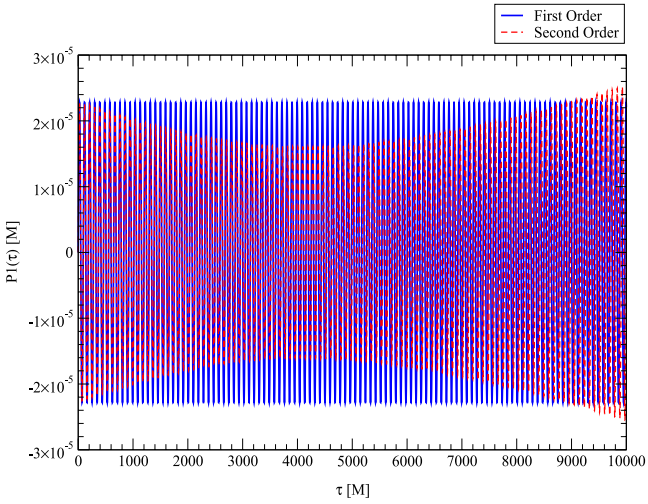

(a) $s_0/(m_0\,r) = 10^{-2}\,,\ a = M$

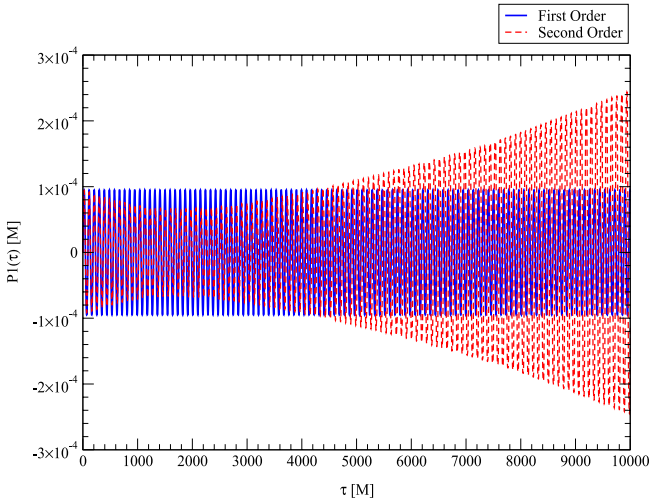

(b) $s_0/(m_0\,r) = 10^{-2}\,,\ a = -M$

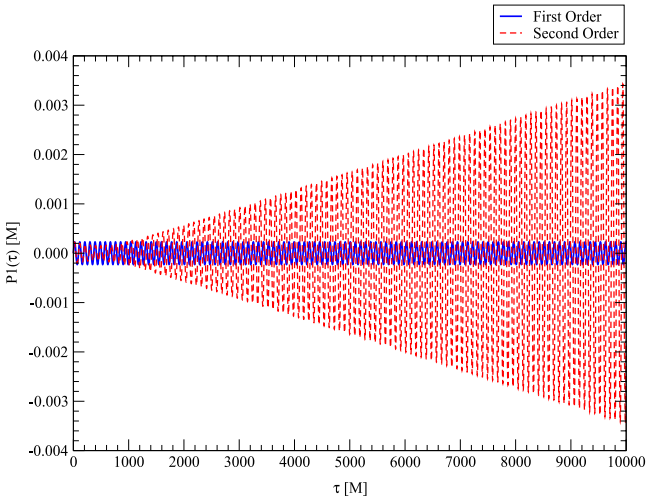

(c) $s_0/(m_0\,r) = 10^{-1}\,,\ a = M$

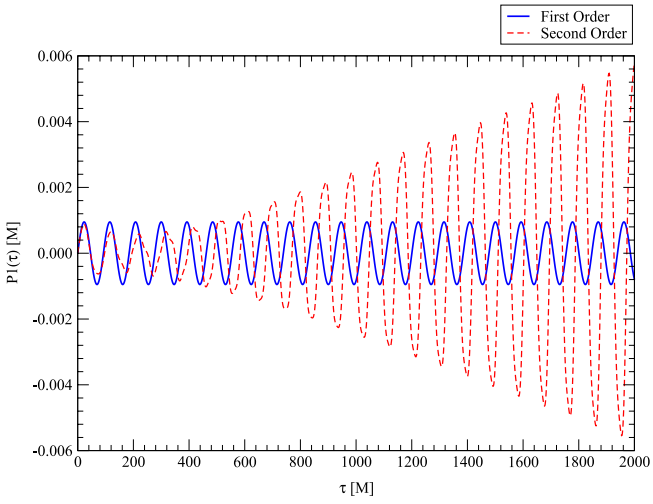

(d) $s_0/(m_0\,r) = 10^{-1}\,,\ a = -M$

FIG. 5 (color online). Radial component $P^1(\tau)$ of the linear momentum for $r = 6M$ and $\hat{\theta} = \hat{\phi} = \pi/4$. (a) shows a slightly growing amplitude due to the second-order contribution in ε for $s_0/(m_0 r) = 10^{-2}$, with a more moderate growth in (b). The amplitude grows much more rapidly for (c) and (d) as $s_0/(m_0 r) = 10^{-1}$.

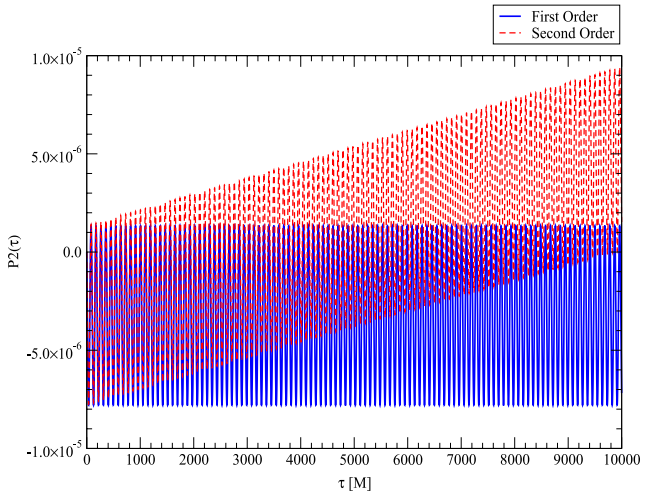

(a) $s_0/(m_0\,r) = 10^{-2}\,,\ a = M$

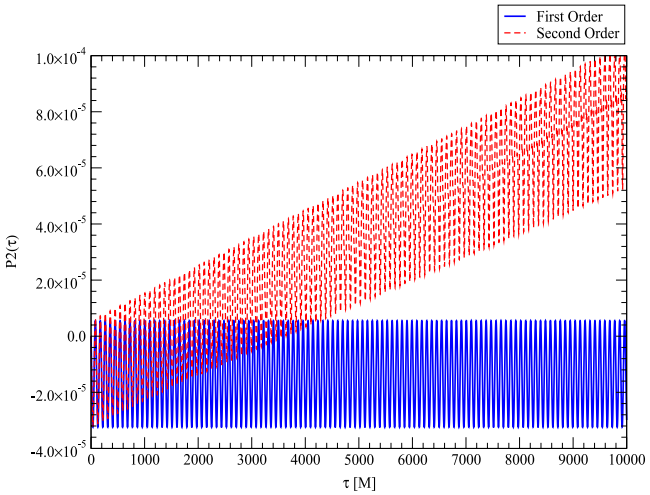

(b) $s_0/(m_0\,r) = 10^{-2}\,,\ a = -M$

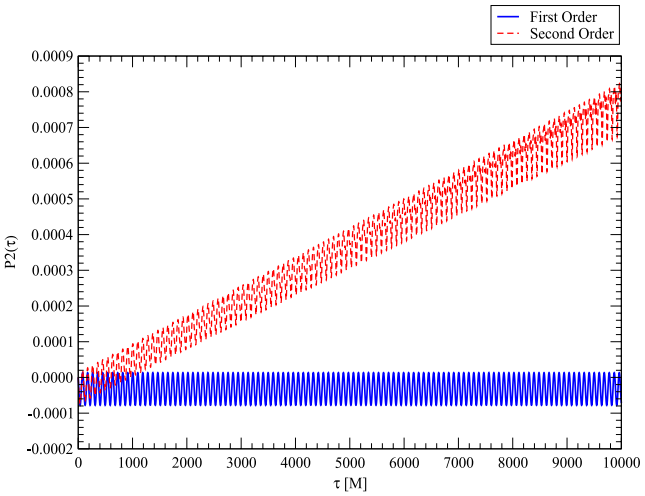

(c) $s_0/(m_0\,r) = 10^{-1}\,,\ a = M$

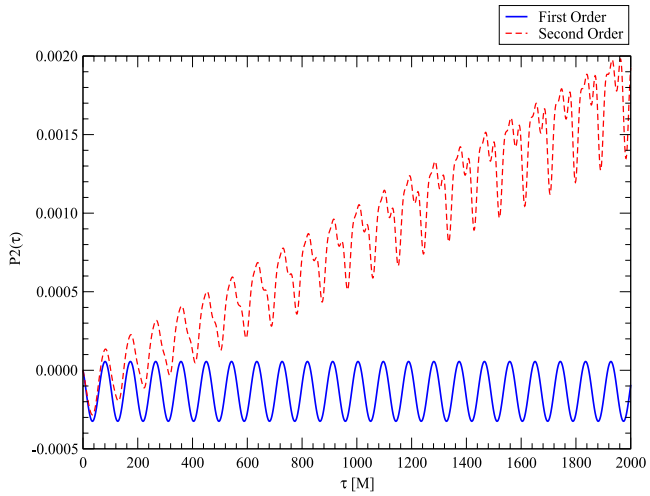

(d) $s_0/(m_0\,r) = 10^{-1}\,,\ a = -M$

FIG. 6 (color online). Polar component $P^2(\tau)$ of the linear momentum for $r = 6M$ and $\hat{\theta} = \hat{\phi} = \pi/4$. The second-order contribution in ε introduces a slight nonzero value in the net magnitude for (a) and (b) with $s_0/(m_0 r) = 10^{-2}$, whose average slope becomes more pronounced for (c) and (d) as $s_0/(m_0 r) = 10^{-1}$.

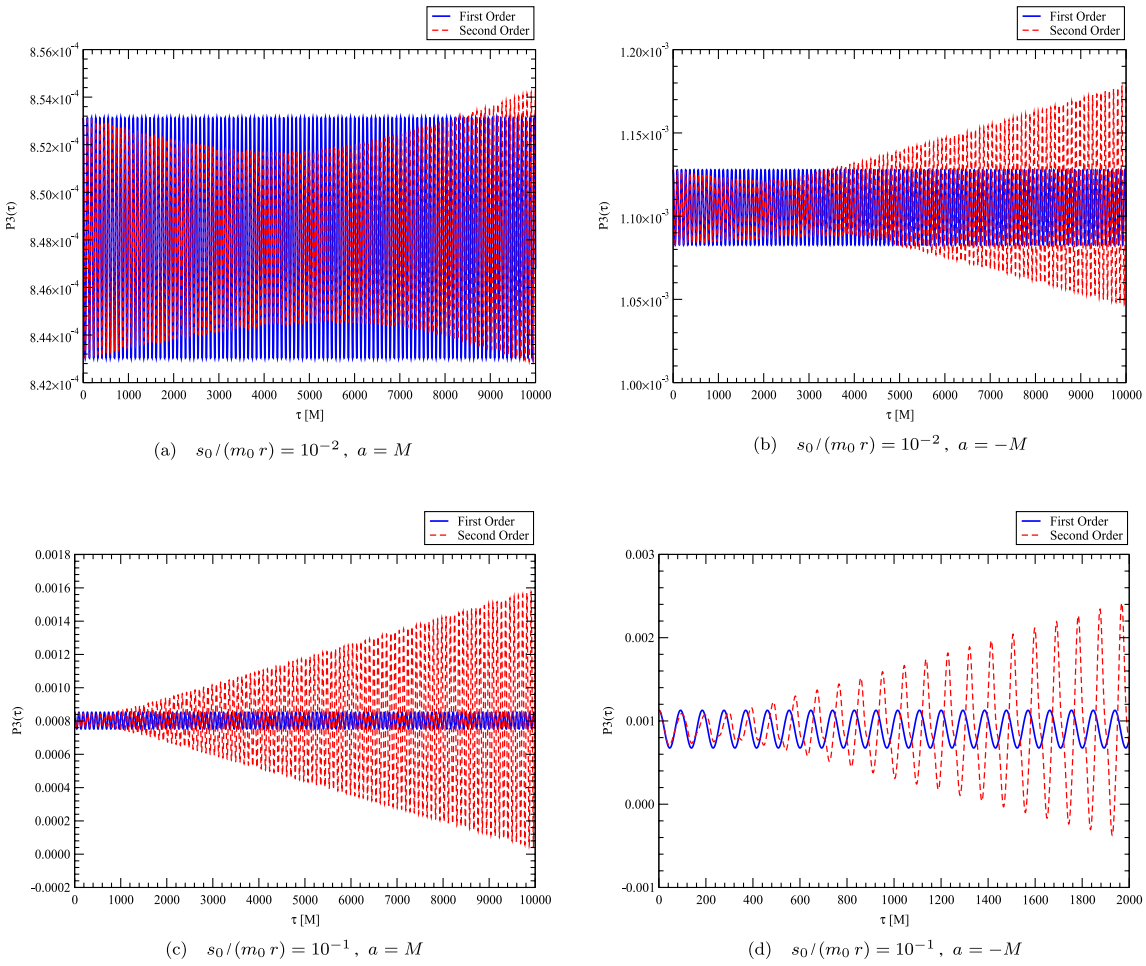

(a) $s_0/(m_0\,r) = 10^{-2}\,,\ a = M$ (b) $s_0/(m_0\,r) = 10^{-2}\,,\ a = -M$

(c) $s_0/(m_0\,r) = 10^{-1}\,,\ a = M$ (d) $s_0/(m_0\,r) = 10^{-1}\,,\ a = -M$

FIG. 7 (color online). Azimuthal component $P^3(\tau)$ of the linear momentum for $r = 6M$ and $\hat{\theta} = \hat{\phi} = \pi/4$. The second-order contribution in ε introduces a slight nonzero change in the amplitude for (a) with $s_0/(m_0 r) = 10^{-2}$, while (b) shows a more moderate growth in amplitude. This growth becomes strongly unbounded for (c) and (d) as $s_0/(m_0 r) = 10^{-1}$.

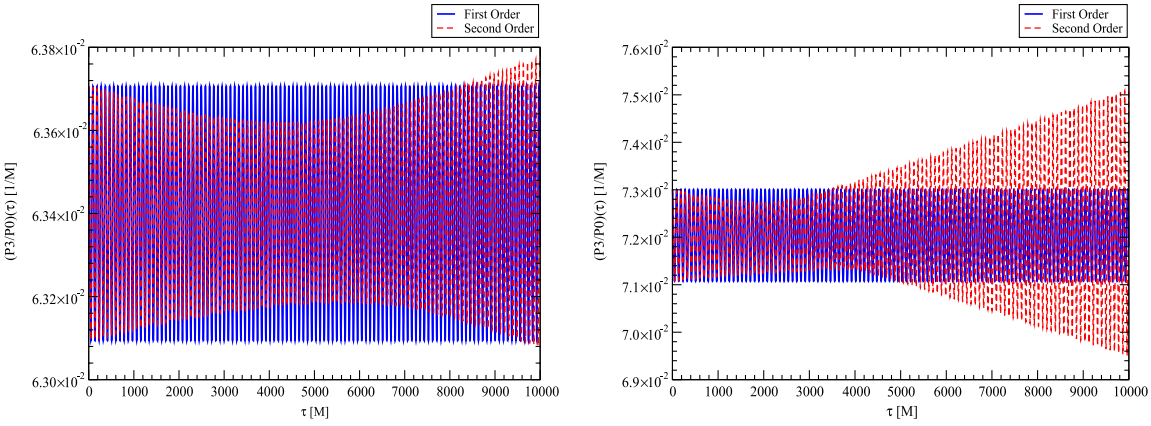

(a) $s_0/(m_0\,r) = 10^{-2}\,,\ a = M$ (b) $s_0/(m_0\,r) = 10^{-2}\,,\ a = -M$

FIG. 8 (color online). Ratio of $P^3(\tau)$ to $P^0(\tau)$ for $r = 6M$ and $\hat{\theta} = \hat{\phi} = \pi/4$. When considering the expression to second order in ε, it is evident from (a) and (b) that the higher-order contribution becomes gradually unbounded compared to the constant ratio given by the first-order contribution in ε.

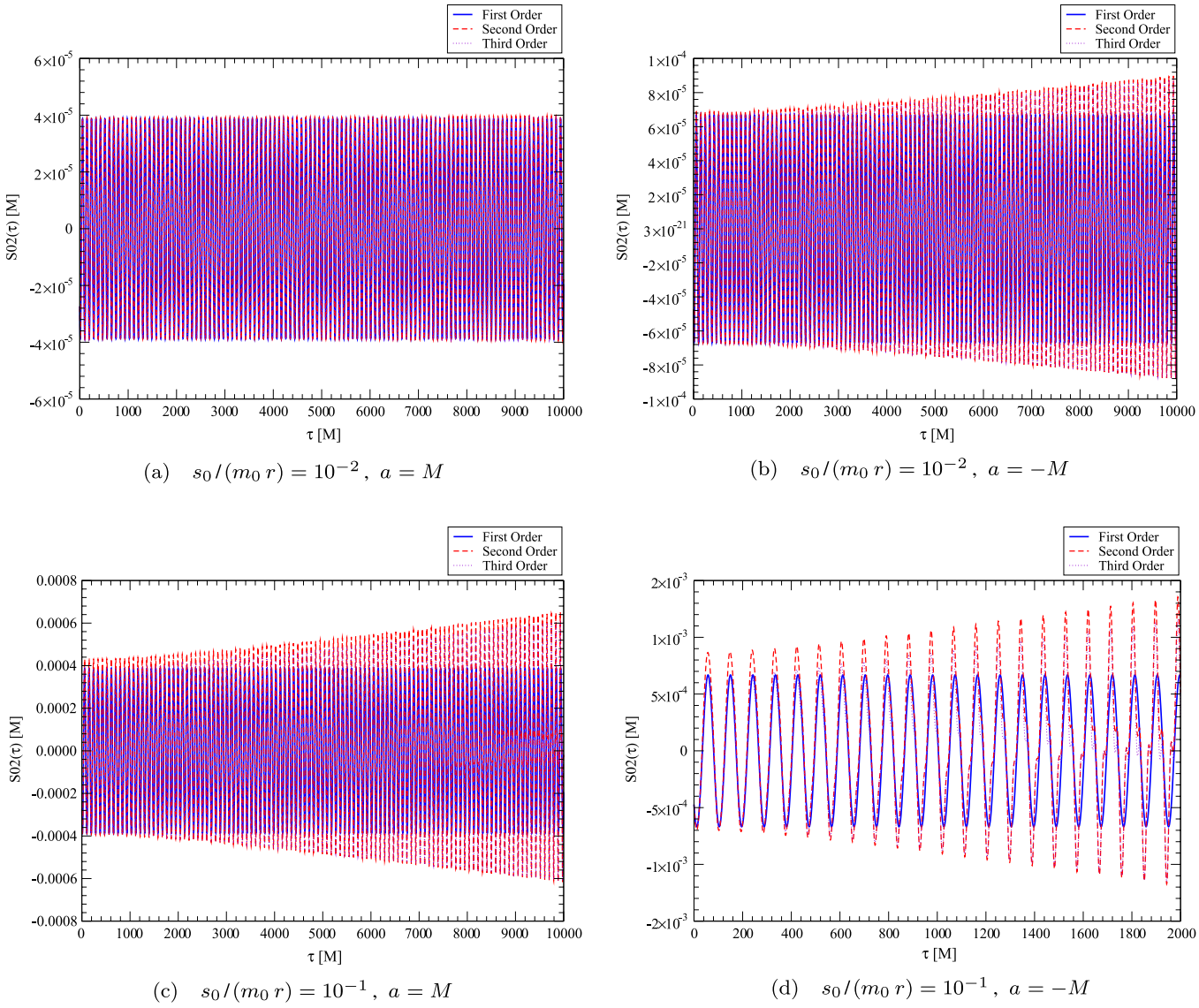

(a) $s_0/(m_0\,r) = 10^{-2}\,,\ a = M$

(b) $s_0/(m_0\,r) = 10^{-2}\,,\ a = -M$

(c) $s_0/(m_0\,r) = 10^{-1}\,,\ a = M$

(d) $s_0/(m_0\,r) = 10^{-1}\,,\ a = -M$

FIG. 9 (color online). The $S^{02}(\tau)$ component of the spin tensor for $r = 6M$ and $\hat{\theta} = \hat{\phi} = \pi/4$. In (a), there is virtually no contribution of the second-order and third-order contributions in ε to the amplitude, while there appears a slight growth in amplitude for (b) due to these contributions. In contrast, (c) and (d) show a noticeable increase in the amplitude as $s_0/(m_0 r) = 10^{-1}$ due to the higher-order contributions in ε.

[1] http://lisa.jpl.nasa.gov.
[2] M. Mathisson, Acta Phys. Pol. **6**, 167 (1937).
[3] A. Papapetrou, Proc. R. Soc. London **209**, 248 (1951).
[4] W. Tulczyjew, Acta Phys. Pol. **18**, 393 (1959); W. G. Dixon, Nuovo Cimento **34**, 317 (1964); J. Madore, Ann. Inst. Henri Poincaré **11**, 221 (1969).
[5] W. G. Dixon, Phil. Trans. R. Soc. A **277**, 59 (1974).
[6] W. G. Dixon, *Isolated Gravitating Systems in General Relativity* (North-Holland, Amsterdam, 1979), Vol. 156.
[7] B. Mashhoon, J. Math. Phys. (N.Y.) **12**, 1075 (1971).
[8] R. Wald, Phys. Rev. D **6**, 406 (1972).
[9] K. P. Tod, F. de Felice, and M. Calvani, Nuovo Cimento Soc. Ital. Fis. B **34**, 365 (1976).
[10] O. Semerák, Mon. Not. R. Astron. Soc. **308**, 863 (1999).
[11] S. Suzuki and K. I. Maeda, Phys. Rev. D **58**, 023005 (1998).
[12] S. Suzuki and K. I. Maeda, Phys. Rev. D **61**, 024005 (1999).
[13] M. D. Hartl, Phys. Rev. D **67**, 024005 (2003).
[14] M. D. Hartl, Phys. Rev. D **67**, 104023 (2003).
[15] Y. Mino, M. Shibata, and T. Tanaka, Phys. Rev. D **53**, 622 (1996).
[16] T. Tanaka, Y. Mino, M. Sasaki, and M. Shibata, Phys. Rev. D **54**, 3762 (1996).
[17] J. Ehlers and E. Rudolph, Gen. Relativ. Gravit. **8**, 197 (1977).
[18] I. Bailey and W. Israel, Ann. Phys. (N.Y.) **130**, 188 (1980).
[19] T. W. Noonan, Astrophys. J. **291**, 422 (1985).

[20] C. Chicone, B. Mashhoon, and B. Punsly, Phys. Lett. A **343**, 1 (2005).
[21] B. Mashhoon and D. Singh, Phys. Rev. D **74**, 124006 (2006).
[22] C. Møller, Commun. Inst. Dublin Adv. Stud., Ser A, 5 (1949).
[23] D. Singh, Gen. Relativ. Gravit. **40**, 1179 (2008).
[24] J. A. Nieto and M. P. Ryan, Nuovo Cimento Soc. Ital. Fis. A **63**, 71 (1981).
[25] M. Mohseni, R. W. Tucker, and C. Wang, Classical Quantum Gravity **18**, 3007 (2001).
[26] S. Kessari, D. Singh, R. W. Tucker, and C. Wang, Classical Quantum Gravity **19**, 4943 (2002).
[27] C. W. Misner, K. S. Thorne, and J. A. Wheeler, *Gravitation* (W. H. Freeman and Company, New York, 1973).
[28] F. Pirani, Acta Phys. Pol. **15**, 389 (1956).
[29] C. Chicone and B. Mashhoon, Classical Quantum Gravity **23**, 4021 (2006).
[30] S. Chandrasekhar, *The Mathematical Theory of Black Holes* (Oxford University, New York, 1992).
[31] G. B. Cook, S. L. Shapiro, and S. A. Teukolsky, Astrophys. J. **424**, 823 (1994).
[32] D. Singh, following Article, Phys. Rev. D **78**, 104029 (2008).